## General Disclaimer

## One or more of the Following Statements may affect this Document

- This document has been reproduced from the best copy furnished by the organizational source. It is being released in the interest of making available as much information as possible.

- This document may contain data, which exceeds the sheet parameters. It was furnished in this condition by the organizational source and is the best copy available.

- This document may contain tone-on-tone or color graphs, charts and/or pictures, which have been reproduced in black and white.

- This document is paginated as submitted by the original source.

- Portions of this document are not fully legible due to the historical nature of some of the material. However, it is the best reproduction available from the original submission.

NASA CR-72482

# ELECTROCHEMICAL CHARACTERIZATION OF NONAQUEOUS SYSTEMS FOR SECONDARY BATTERY APPLICATION

by

M. Shaw, O. A. Paez, D. A. Lufkin



prepared for

NATIONAL AERONAUTICS AND SPACE ADMINISTRATION

CONTRACT NO. NAS 3-8509



NINTH QUARTERLY REPORT
MAY - JULY 1968

WHITTAKER CORPORATION
RESEARCH & DEVELOPMENT/SAN DIEGO
3540 Aero Court
San Diego, California 92123

CR-72482

# NINTH QUARTERLY REPORT

# ELECTROCHEMICAL CHARACTERIZATION OF NONAQUEOUS SYSTEMS FOR SECONDARY BATTERY APPLICATION

May - July 1968

by

M. Shaw, O. A. Paez, D. A. Lufkin

prepared for

NATIONAL AERONAUTICS AND SPACE ADMINISTRATION

August 16, 1968

CONTRACT NAS 3-8509

Technical Management
Space Power Systems Division
National Aeronautics and Space Administration
Lewis Research Center, Cleveland, Ohio
Mr. Robert B. King

WHITTAKER CORPORATION
RESEARCH & DEVELOPMENT/SAN DIEGO
3540 Aero Court
San Diego, California 92123

TABLE OF CONTENTS

TABLE OF FIGURES

COULOMBS DISCHARGE vs COULOMBS CHARGE

# ELECTROCHEMICAL CHARACTERIZATION OF NONAQUEOUS SYSTEMS FOR SECONDARY BATTERY APPLICATION

by

M. Shaw, O. A. Paez, D. A. Lufkin

## ABSTRACT

The electrochemical characterization of 950 nonaqueous battery systems, with regard to secondary battery application, has resulted in a list of twenty-four recommended positive electrolyte systems. Additional evaluation of these twenty-four systems has included wet stand compatibility tests and solubility measurements of charged state material on wire electrodes.

A program, using sintered type electrodes, to measure discharge capacity as a function of charge inputs for the recommended systems has been initiated during this reporting period. The results on nineteen systems are presented in this report.

## SUMMARY

A program, using sintered type electrodes, designed to evaluate the twenty-four recommended systems has been initiated during this reporting period. The method used in this program involves the measurement of the discharge capacity as a function of charge input. The tests are carried out at constant current under conditions of excess electrolyte. The results provide information on the utilization efficiency, defined as the ratio of specific discharge capacity to specific charge capacity as well as on the system reversibility as indicated by the voltage separation between charge and discharge plateaus. Tests on nineteen systems have been completed thus far. The results have provided information useful as a basis for selecting the most promising of the twenty-four systems from the standpoint of secondary battery application. Tentative recommendations have been made in this report, however final choice of the most promising systems and an overall evaluation will be made when tests on all twenty-four systems are completed.

# I. INTRODUCTION

Previous work (Ref. 1) has shown that the compatibility test on wire electrodes was not a reliable method for choosing the best of the 24 recommended positive-electrolyte systems. This test consisted of sweep charge and constant current discharge of wire electrodes. Because of the varying amounts of charged state material introduced into the electrolyte, and the uncontrolled coulombic input inherent to the sweep method, it was impossible to evaluate the data on a comparable basis. It was therefore decided to measure discharge capacity as a function of known and variable charge inputs using sintered-type electrodes.

Percent utilization, as used here, is defined as the ratio of the specific discharge capacity to the specific charge capacity, both expressed in coulombs per square centimeter. A plot of the discharge capacity (coulombs delivered) versus the charge capacity (coulombs passed) for different charge inputs should give a straight line whose slope represents the percent utilization. If the coulombic input exceeds that required for the desired charge reaction, so that the incremental coulombs are utilized for some other anodic reaction the product of which is not dischargeable, then the plot will depart from linearity and ultimately reach a slope of zero. This tendency towards a decreasing slope, or towards an asymptotic value, will also be indicated if the charged material becomes unavailable for discharge, either due to dissolution, material detachment, or deactivation of any kind. Also, the charge process may be more efficient than the discharge process, so that a lesser amount of charged material is discharged, this becoming more pronounced at the greater depths of conversion (higher charge capacity values). Whatever the mechanism, the information obtained from plots of discharge capacity against charge capacity (percent utilization and extent of non-linearity) will be of value in choosing the most desirable systems.

## II. RESULTS AND DISCUSSION

Charge-discharge tests on porous sintered metal electrodes on 24 selected systems have been initiated during this reporting period. The results on nineteen systems tested thus far are presented in this report. A list of these systems and their utilization efficiencies are summarized in Table I. Charge-discharge plots showing the coulombs delivered as a function of the charge input, and representative voltage-time curves are included in the figures. Discharge capacities were measured at a break in the discharge plateau at an appropriate cutoff voltage within 0.5 volt negative to the rest potential. In some instances, the knee of the discharge plateau became less well-defined as the tests progressed, possibly due to increasing effective electrode area on cycling. In such cases the cutoff voltages were taken at potentials consistent within a given triplication of measurements.

Where the reduction of dissolved electroactive material was sufficient to cause a prolonged discharge, the cutoff was set at 120% of charge. Prolonged discharge occurs when the discharge current density is less than the limiting diffusion current for a given concentration of dissolved electroactive material. In this case a drop-off in the discharge plateau occurs gradually as a function of the concentration of electroactive material in the bulk solution. In most of the systems, the concentration of electroactive material in the saturated electrolyte is sufficient to maintain diffusion currents of 1 $ma/cm^2$. If the reduction of dissolved material takes place at potentials coinciding with the discharge of solid material, the discharge may be masked or incomplete, and accordingly build up on the electrode as cycling is continued. It is likely in this case that higher limiting current values can result, depending on the dissolution rate of solid material on the electrode surface.

TABLE I

UTILIZATION EFFICIENCY

| System | 1 ma/cm$^2$ | 5 ma/cm$^2$ |
|---|---|---|
| AgO/BL-LiCl + $AlCl_3$ | 82 | 87 |
| Cu/AN-LiPF + $KPF_6$ | 120 | 120 |
| Cu/DMF-$LiPF_6$ | 120 | 42 |
| $CuF_2$/DMF-$LiPF_6$ | 120 | 72 |
| $CuF_2$/PC-$LiPF_6$ | 75 | 5 |
| $CuCl_2$/AN-$LiPF_6$ | 120 | 120 |
| $CuCl_2$/DMF-$LiPF_6$ | 120 | 100 |
| $CuCl_2$/PC-$LiClO_4$ | 90 | nil |
| Zn/AN-$LiClO_4$ | 120 | 7 * |
| Zn/DMF-$LiClO_4$ | 120 | 4 * |
| Zn/DMF-$LiPF_6$ | 120 | 56 * |
| Zn/DMF-$KPF_6$ (.75 m) | 120 | 69 |
| Zn/DMF-$KPF_6$ (2.0 m) | 120 | 47 |
| Zn/BL-$KPF_6$ | 120 | 12 *, 77 ** |
| Zn/PC-$KPF_6$ | 120 | 12 |
| Cd/DMF-$KPF_6$ | 120 | 46 *, 120 ** |
| Cd/DMF-$LiBF_4$ | 120 | 4 * |
| Cd/DMF-$LiClO_4$ | 120 | 53 |
| Cd/BL-$KPF_6$ | 120 | 54 * |

AN - Acetonitrile
DMF - Dimethylformamide
BL - Butyrolactone
PC - Propylene carbonate

* - calculated from best straight line through all points up to 5 coul/cm$^2$ charge input.

** - calculated for 10 coul/cm$^2$ charge input.

The highest metal ion concentration measured in previous work was 4 x $10^{-2}$ M. The limiting current for this concentration for a two electron change at a planar electrode is less than 4 ma/cm$^2$, based on known results in aqueous solution. Likewise, the contribution to the transition time for a current density of 5 ma/cm$^2$ is of the order of 50 seconds, or less than 3% of the largest charge input (10 coul/cm$^2$) in these tests. Consequently a linear relationship between the coulombs passed during charge and discharge tests must represent a measure of the utilization efficiency for discharge of product formed during the charge reaction.

A slope of unity indicates 100% efficiency. A decreasing slope indicates that the charge material becomes unavailable for discharge either due to dissolution, material detachment, or deactivation of some kind. Quantities greater than 100% indicate contribution due to dissolved material, or activation with cycling, of charged solid material.

Almost all systems show a prolonged discharge at the low current density (1 ma/cm$^2$) giving utilization efficiencies greater than 120%. In these instances, triplicate measurements were taken only for the smallest charge input (0.10 coul/cm$^2$), where discharge was allowed to continue until 0.20 coul/cm$^2$ was passed. Single tests on all succeeding measurements at 1 ma/cm$^2$ were made allowing the discharge to proceed to 120% of the charge input. A minimum of three tests was made at all charge inputs where a drop-off in the voltage of the discharge plateau was evident prior to the 120% stopping point, except in those instances mentioned in the text.

In the charge-discharge plots, the circles represent the average of a minimum of three discharge tests unless otherwise indicated. The variation within each set of tests is shown by the vertical lines, the cross bars indicating individual test results. The sequence of a given test result

within a set of measurements is indicated by the number next to each bar. In some cases the reproducibility of three tests lies within the range of the circle.

1. Silver Oxide Electrode in Butyrolactone-$LiCl + AlCl_3$

Initial discharge for this system was nil. Immediate polarization on discharge was greater than 0.8 volts. Less than 15% utilization of the 10 coul/$cm^2$ electroformed silver oxide was recovered at a current density of 3 ma/$cm^2$. The regular testing procedure was followed after these initial discharge tests. Charge-discharge plots for this system are linear with a slope indicating a utilization efficiency better than 80% for both the 1 and 5 ma/$cm^2$ tests. These are shown as Figures 1 and 2. The voltage separating charge and discharge plateaus at 1 and 5 ma/$cm^2$ are 0.3 and 0.5 volts respectively. Results indicate the discharge of solid state material formed during the charge cycle at all capacities. This system is recommended for further study.

2. Copper Electrode in Acetonitrile-$LiPF_6$ + $KPF_6$

This system exhibited prolonged discharge at all charge input values for both 1 and 5 ma/$cm^2$. The voltage separating the charge and discharge plateaus at 5 ma/$cm^2$ was 0.12 v, indicating high electrochemical activity for dissolved material. Examination of the electrode showed that extensive disintegration had taken place, with only a small portion remaining attached to the lead wire contact. Results indicate a high contribution to the discharge due to dissolved electroactive copper material, and loss of electrode integrity on charge. This system should be eliminated from further study.

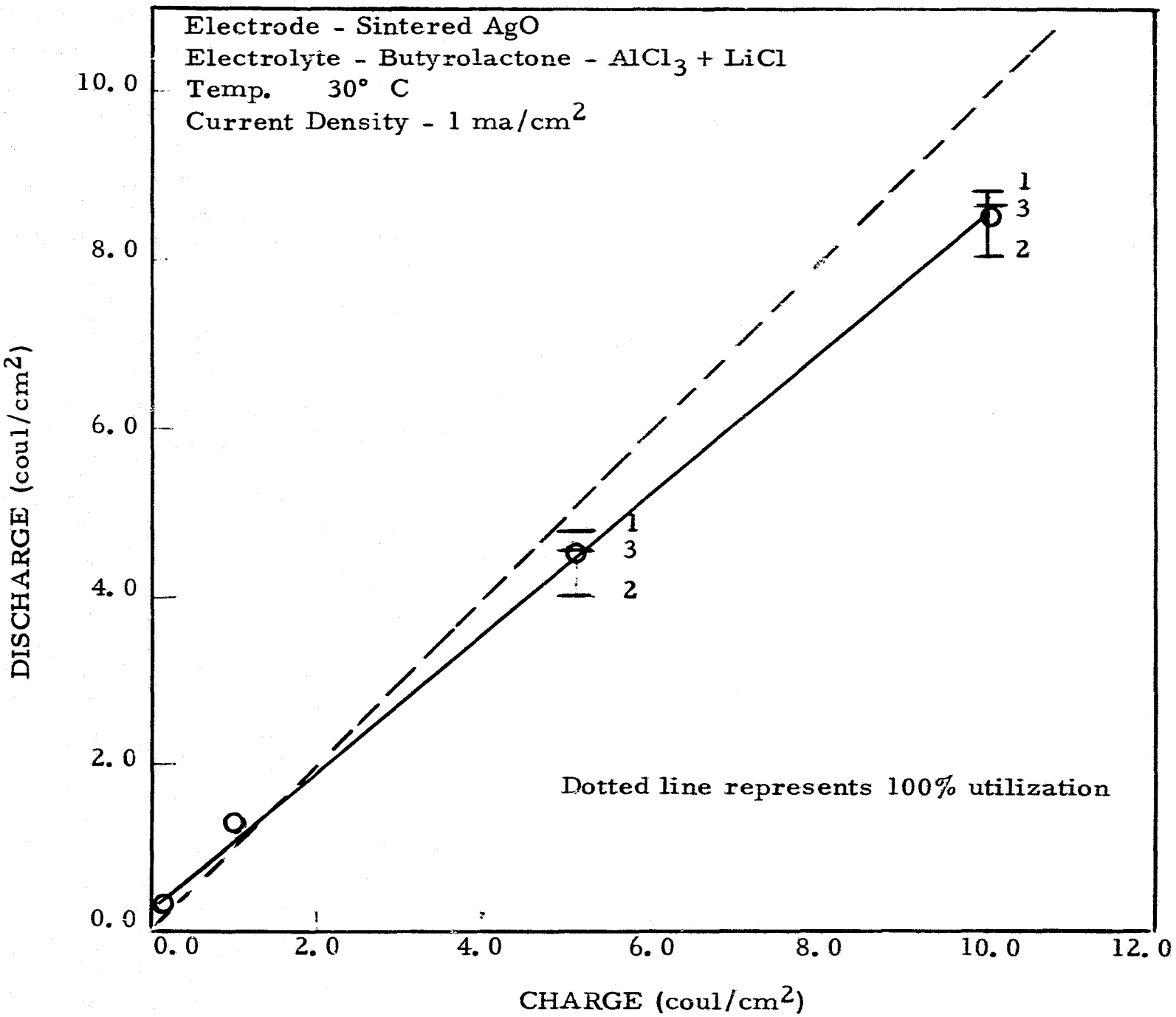


Figure 1. Coulombs delivered as a function of coulombs passed

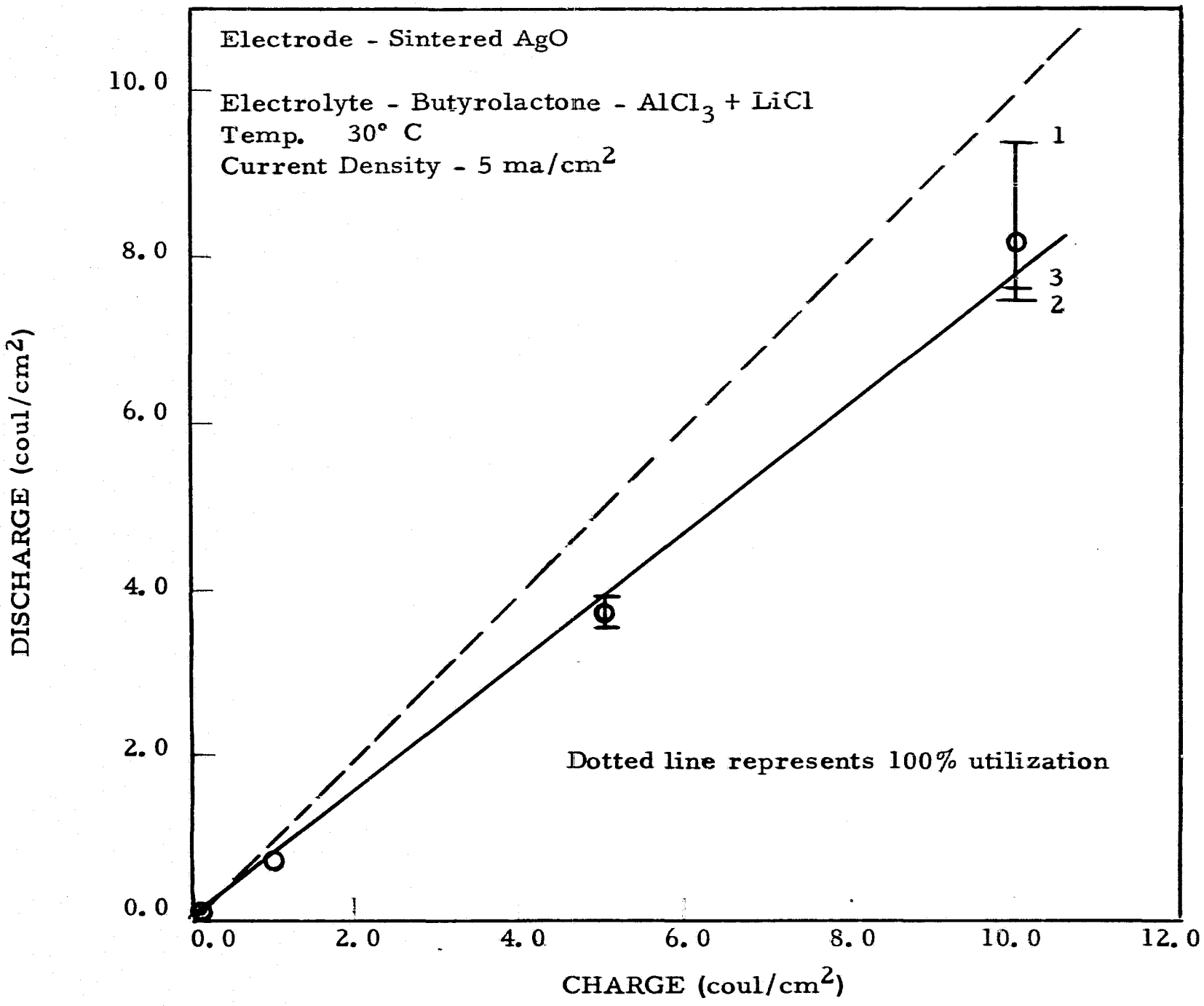


Figure 2. Coulombs delivered as a function of coulombs passed

3. Copper Electrode in Dimethylformamide-$LiPF_6$

This system showed prolonged discharge (utilization efficiency greater than 120%) for the 1 ma/$cm^2$ tests. The voltage separating the charge and discharge plateau was only 0.03 volts at 1 ma/$cm^2$ indicating high electrochemical activity for dissolved material. A drop-off in the discharge plateau occurred only for the 5 ma/$cm^2$ tests where the voltage separation was 0.1 volts. The charge-discharge plot is shown in Figure 3.

The average utilization efficiency for all charge inputs at 5 ma/$cm^2$ is 42%. Reproducibility is good for the two lowest charge input values, however a spread from 1.3 to 4.8 coul/$cm^2$ results at the 5 coul/$cm^2$ charge input, with values increasing with cycling. A similar effect is noted at the 10 coul/$cm^2$ charge input. Only two tests were made at this point since loss of contact caused by electrode disintegration occurred after the second discharge cycle. Examination of several pieces of the electrode, which had fallen to the bottom of the cell, revealed a large hole pattern had developed in the central portion of the electrode. This system should be eliminated from further study.

4. Copper Fluoride Electrode in Dimethylformamide-$LiPF_6$

The test procedure remained the same except that an initial discharge is introduced to bring the electrode to an initial discharged state.

Discharge of active material occurred readily for the $CuF_2$/DMF-$LiPF_6$ system at 5 ma/$cm^2$. The discharge time to a cutoff voltage of - 0.6 v corresponded to 20 coul/$cm^2$, which was better than 80% utilization based on weight gain measurements for a controlled electrode. The regular test procedure was then followed after this initial discharge.

Prolonged discharge (utilization efficiency greater than 120%) occurred for

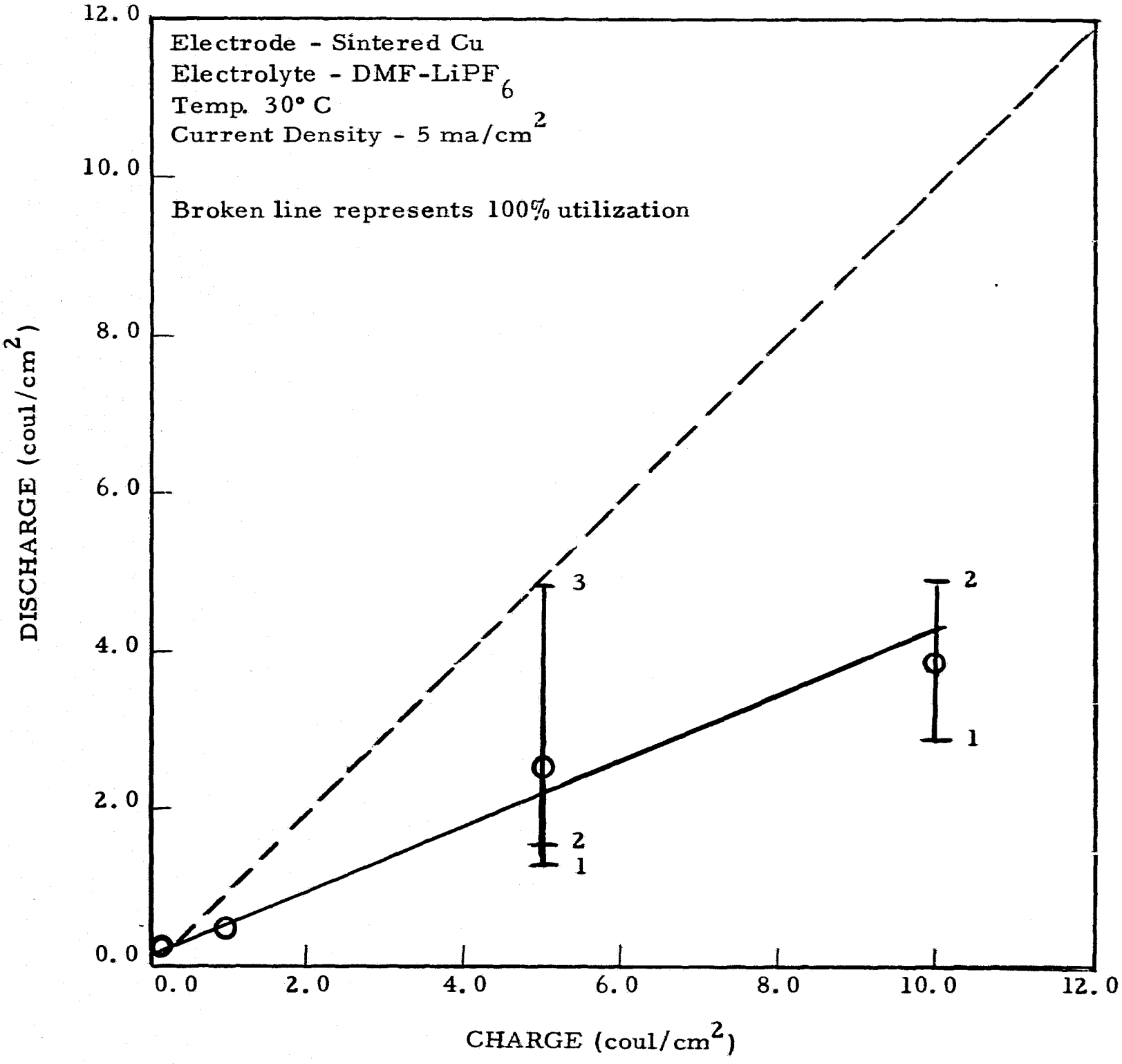


Figure 3. Coulombs delivered as a function of coulombs passed

all tests at 1 ma/cm$^2$. The charge-discharge plot for the 5 ma/cm$^2$ tests is shown in Figure 4. The utilization efficiency based on the best straight line through all the points is 74%. Polarization between charge and discharge plateaus is 0.3 volts. The discharge curve for the largest charge input is shown in Figure 5. Further testing of this system is recommended.

5. Copper Fluoride Electrode in Propylene carbonate-$LiPF_6$

Initial discharge of chemoformed fluoride material for the $CuF_2$/PC-$LiPF_6$ system was nil. A discharge plateau resulted only for currents less than 0.5 ma/cm$^2$. However, charge-discharge curves at 1 ma/cm$^2$ revealed measurable charge utilization and therefore the regular testing procedure was followed. The time-voltage curves showed polarization between charge and discharge plateaus of 0.5 and 1.2 volts respectively for the 1 and 5 ma/cm$^2$ tests. The charge-discharge plots (Figures 6 and 7) also show strong dependence on current density, giving an average utilization efficiency of 75% at 1 ma/cm$^2$ and 5% for the 5 ma/cm$^2$ tests. Only one point was obtained at the 10 coul/cm$^2$ charge input due to separation at the wire lead-electrode junction. This is one of the few systems in which the discharge at the 1 ma/cm$^2$ current density is not masked by prolonged discharge of dissolved active material. It is likely that the chemoformed fluorination product on the electrode surface is a controlling factor affecting the charge-discharge process. Further characterization of this system is in order.

6. Copper Chloride Electrode in Dimethylformamide-$LiPF_6$

Initial discharge of the chemoformed copper chloride electrode at 4 ma/cm$^2$ corresponded to 21 coul/cm$^2$. The regular testing procedure was followed after this initial test.

Tests on this system showed a variation in the charge and discharge

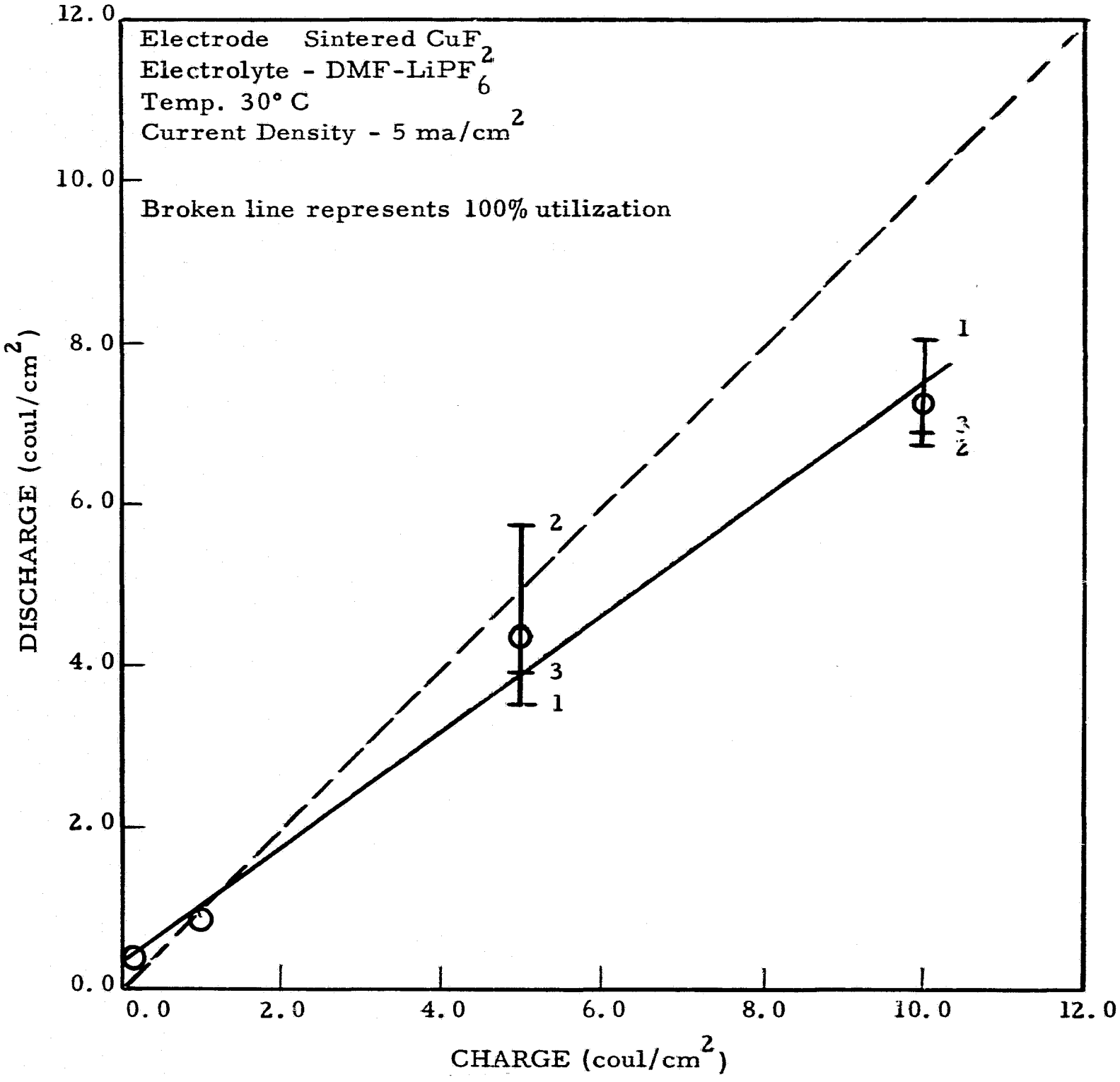


Figure 4. Coulombs delivered as a function of coulombs passed

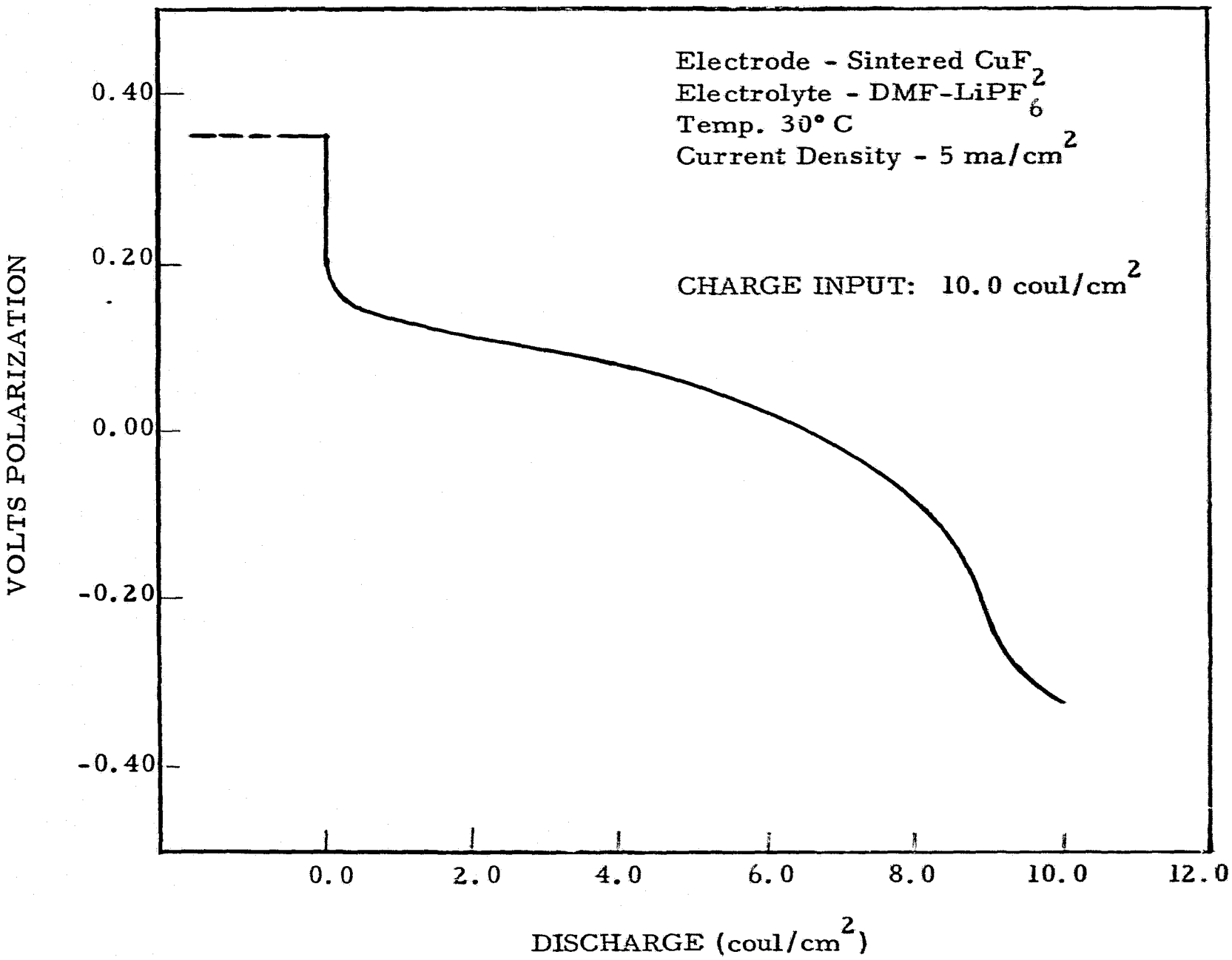


Figure 5. Discharge curve for $CuF_2$/DMF-$LiPF_6$

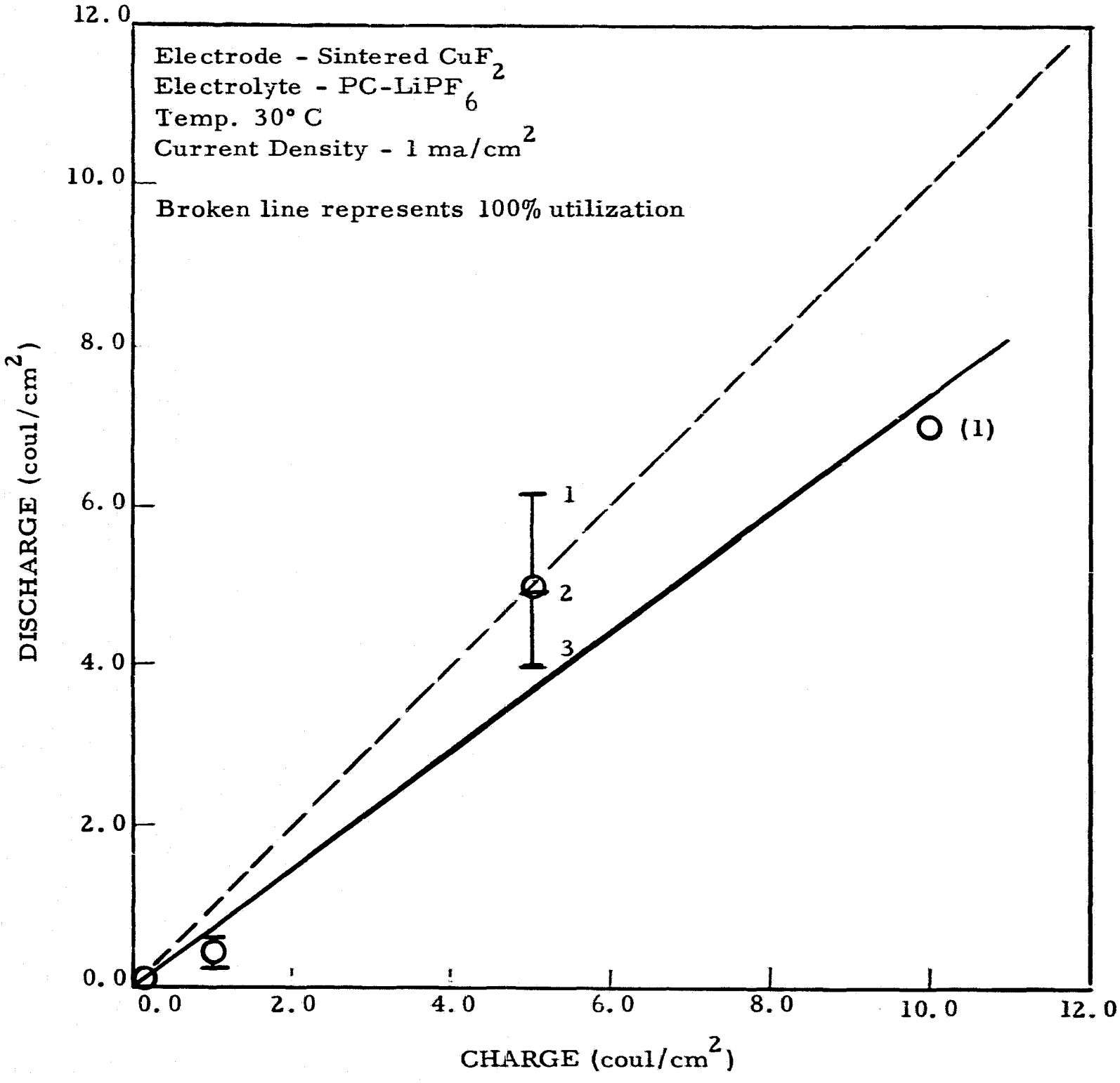


Figure 6. Coulombs delivered as a function of coulombs passed

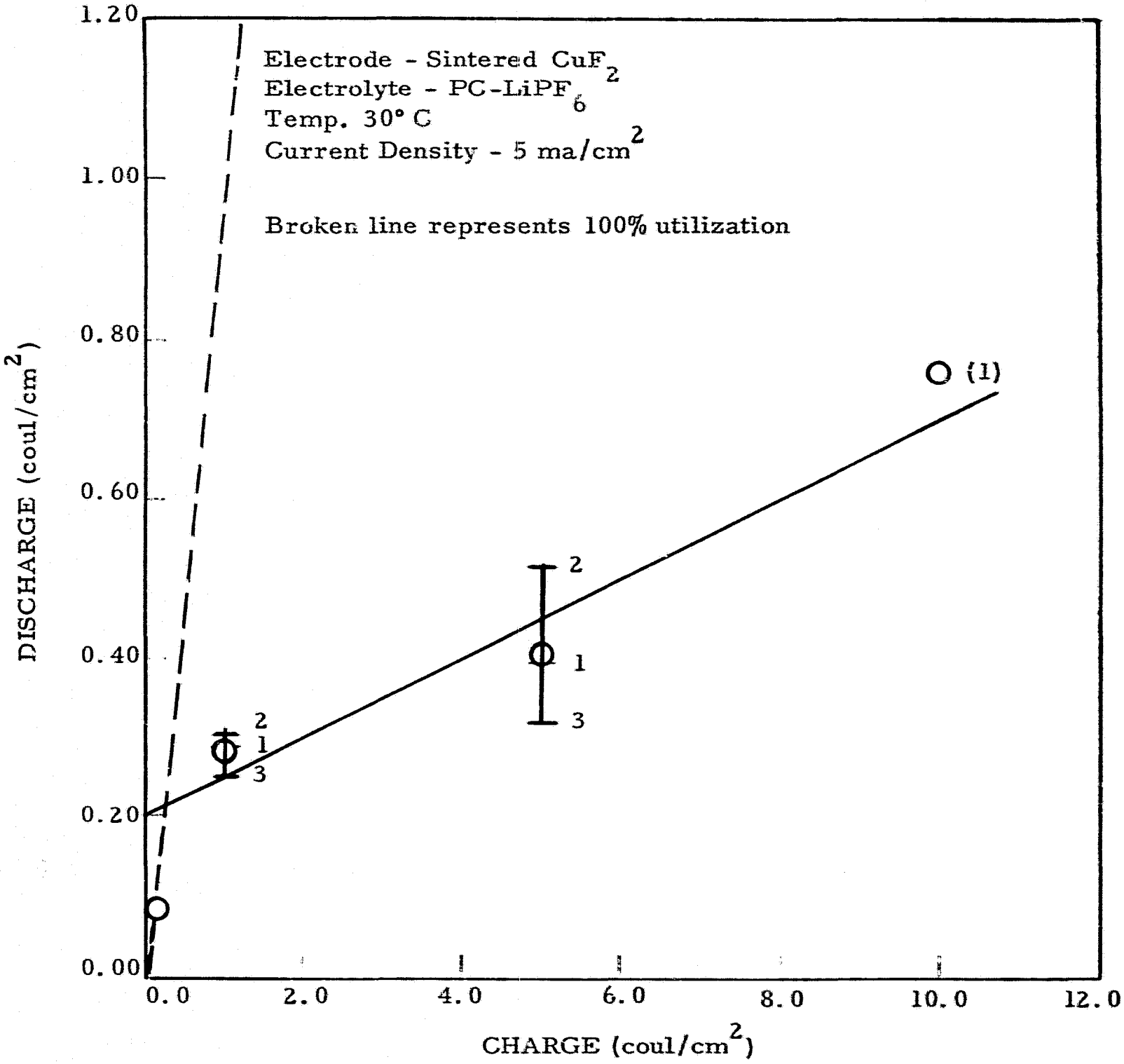


Figure 7. Coulombs delivered as a function of coulombs passed

potential for the first few charge input values. During this time both the charge and discharge plateaus occurred at positive potentials. The tests at 1 ma/cm$^2$ showed a two plateau charge at + 0.2 and + 0.4 volts, with a discharge at + 0.2 volts, with about 50% utilization efficiency at 0.10 coul/cm$^2$ charge. The 5 ma/cm$^2$ tests for the 0.10 coul/cm$^2$ charge showed a single charging plateau at + 0.25 volts with no discharge. A second charging plateau was observed at + 0.7 volts (at the 1.0 coul/cm$^2$ charge) with about 20% utilization. Similar results occurred for 1 ma/cm$^2$ at the 1 coul/cm$^2$ test. These effects disappeared after an overnight stand whereupon all tests at 1 ma/cm$^2$ showed prolonged discharge, and only single charge plateaus were observed for both high and low current densities. The remainder of the tests at 5 ma/cm$^2$ showed two discharge plateaus within - 0.3 v relative to the reference electrode, with overall utilization varying between 80 and 130%, indicating a high contribution due to dissolved material. The charge-discharge plot for the 5 ma/cm$^2$ tests is shown in Figure 8. The results suggest an effect due to residual chloride material remaining within the pores of the electrode from the initial discharge of the chemoformed copper chloride. The chloride ion would be expected to diffuse gradually to the bulk solution because of the high solubility (greater than 2 m) of LiCl in DMF. Further testing with controlled chloride ion concentration is required to clarify these results.

## 7. Copper Chloride Electrode in Acetonitrile-$LiPF_6$

Initial discharge of this system occurred readily at 5 ma/cm$^2$, indicating greater than 90% utilization of the chemoformed material. The regular tests which followed this initial discharge, showed no drop-off in the discharge plateau for either the 1 or 5 ma/cm$^2$ tests. The voltages separating the charge and discharge plateaus were 0.3 and 0.5 volts for the low and high current densities respectively. The results are similar to those observed for the Cu/AN-$LiPF_6$ + $KPF_6$ system and suggest that diffusion of residual chloride ion away from the electrode surface occurs

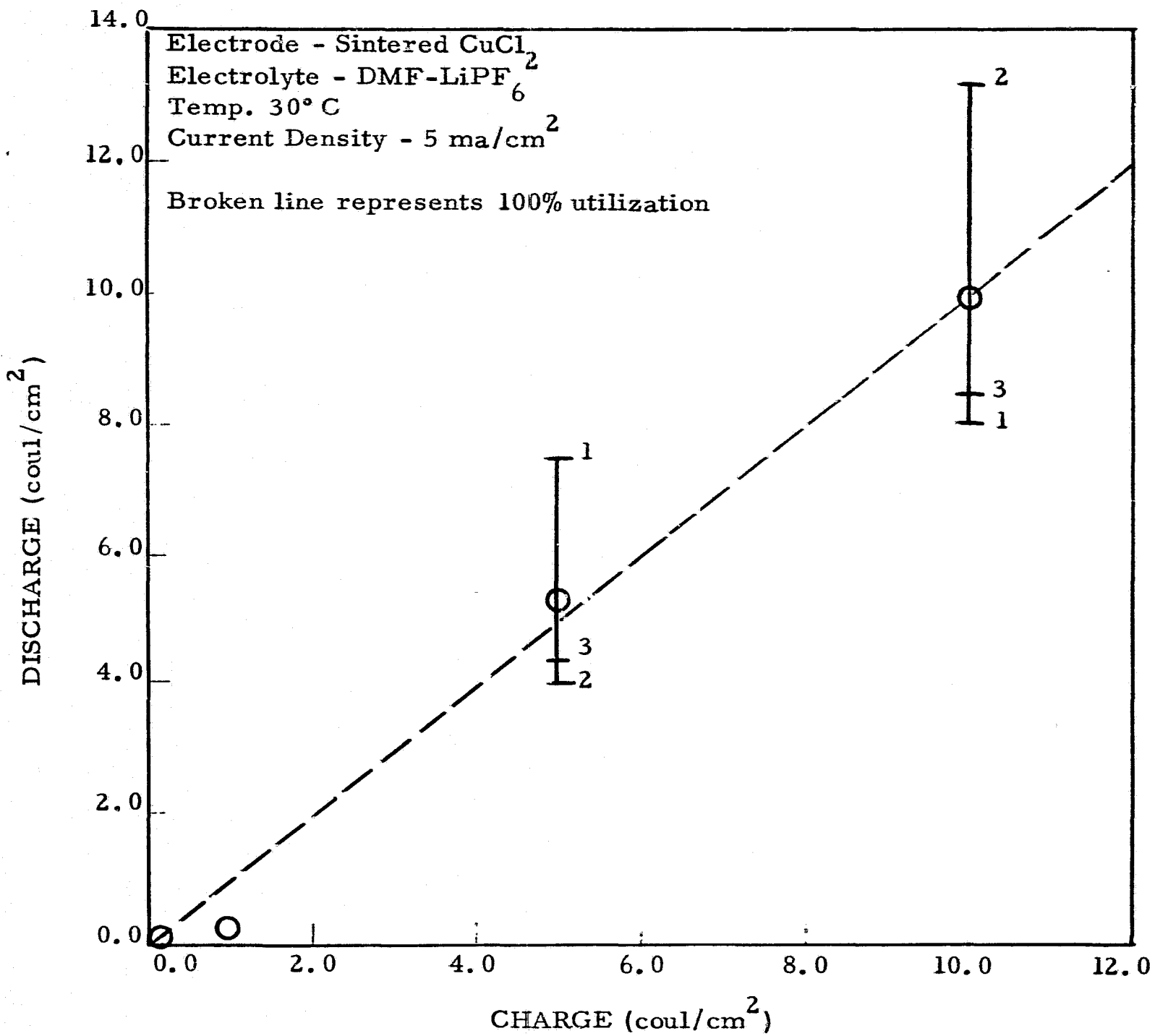


Figure 8. Coulombs delivered as a function of coulombs passed

rapidly, most of it taking place probably during the preconditioning phase of the test procedure. This system is not recommended for further study.

8. Copper Chloride Electrode in Propylene carbonate-$LiClO_4$

Initial discharge of chemoformed copper chloride in this electrolyte was poor. Electrode polarization, at current densities greater than 1 ma/cm$^2$, was more than 1 volt and therefore no measure of active chloride material was obtained. The regular testing procedure was followed after these initial tests.

Prolonged discharge for the 1 ma/cm$^2$ tests occurred at charge inputs of 0.10 and 1.0 coul/cm$^2$, while drop-offs in the discharge plateau occurred for the 5 and 10 coul/cm$^2$ tests. No tests at 5 ma/cm$^2$ were completed since electrode polarization greater than 1 volt for both charge and discharge cycles was observed. The voltage separating the charge and discharge plateaus for the 1 ma/cm$^2$ tests was initially greater than 0.7 v, but then began to decrease with cycling during the 5 coul/cm$^2$ tests, and was less than 0.4 v for the 10 coul/cm$^2$ test. Only one test at 1 ma/cm$^2$ was completed at this highest charge input due to loss of contact as a result of electrode disintegration.

The charge-discharge plot for this system is shown in Figure 9. The average utilization efficiency for the three tests at 5 coul/cm$^2$ is 84% while the point at 10 coul/cm$^2$ corresponds to 96%. This system merits further study in view of the improvement of the charge-discharge characteristics with cycling, and the high utilization efficiency.

9. Zinc Electrode in Acetonitrile-$LiClO_4$

This system showed prolonged discharge at 1 ma/cm$^2$ with relatively no polarization separating the charge and discharge plateaus, indicating, high

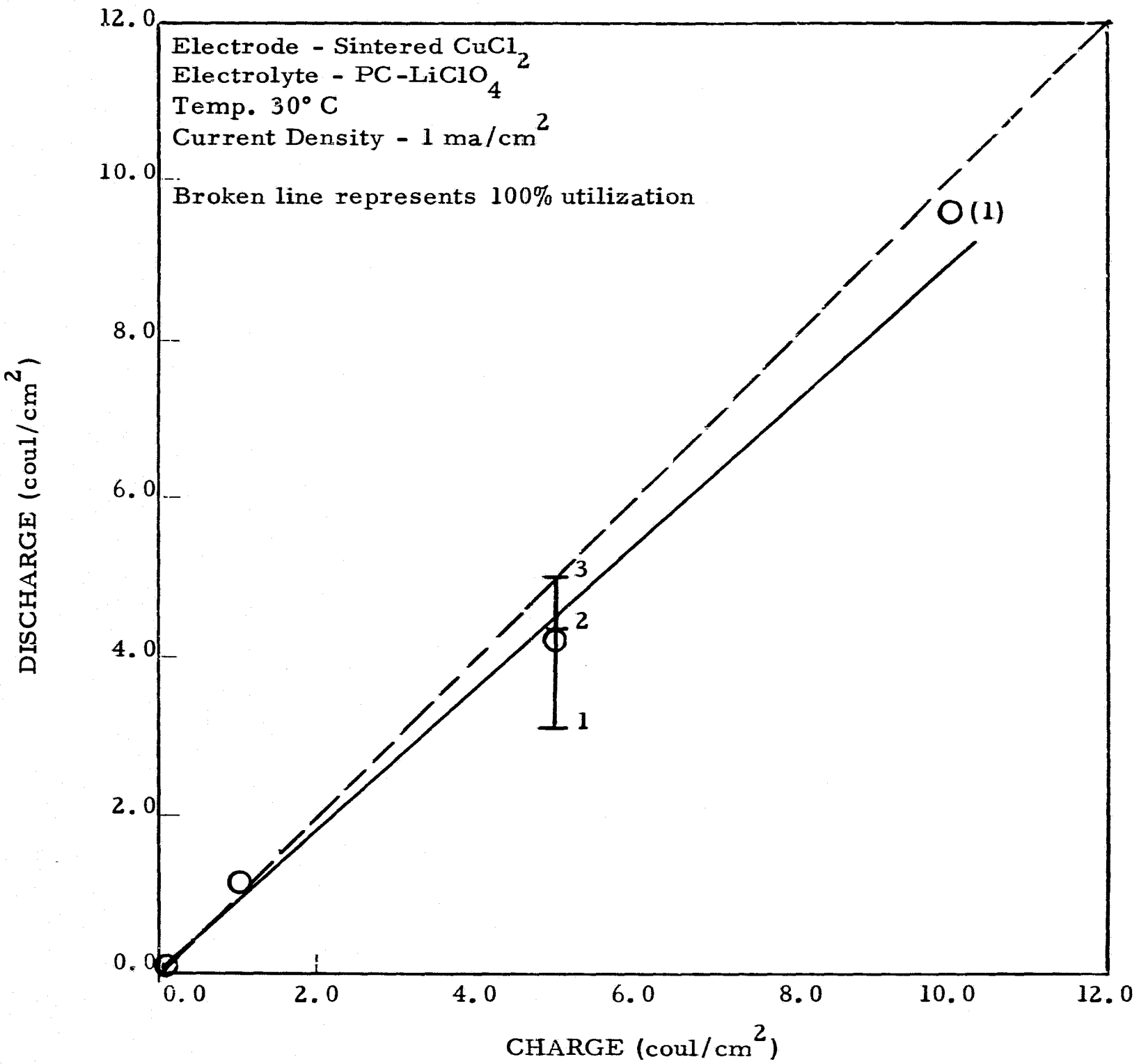


Figure 9. Coulombs delivered as a function of coulombs passed

electrochemical activity for dissolved active material.

The charge-discharge plot for this system (Figure 10) for the 5 ma/cm$^2$ tests shows discharge capacities less than 0.8 coul/cm$^2$ at all charge inputs. These results indicate poor utilization of solid state active material. No further tests are recommended.

10. Zinc Electrode in Dimethylformamide-$LiClO_4$

Test results were similar to those for Zn/AN-$LiClO_4$. The charge-discharge plot is shown in Figure 11. This system is not recommended for further tests.

11. Zinc Electrode in Dimethylformamide-$LiPF_6$

The system Zn/DMF-$LiPF_6$ shows prolonged discharge with low polarization at 1 ma/cm$^2$ indicating high electrochemical activity for dissolved material. The utilization efficiency at 5 ma/cm$^2$, while linear up to the 5 coul/cm$^2$, is less than 60% and then tends to drop off to an average of 37% at 10 coul/cm$^2$. The charge-discharge plot is shown in Figure 12. The results indicate that charging of this electrode to higher charge inputs proves detrimental to its utilization efficiency. This system does not merit further study.

12. Zinc Electrode in Dimethylformamide-$KPF_6$

Charge-discharge tests were carried out in two electrolyte concentrations at 0.75 m and 2.0 m. Both systems show prolonged discharges at 1 ma/cm$^2$ with low polarization, indicating activity for dissolved material. At 5 ma/cm$^2$, the voltage separating the charge and discharge plateaus was 0.3 v for the lower concentration, and 0.6 v for the high concentration, as seen in Figure 13. A pronounced cycling effect is evident in the charge-discharge

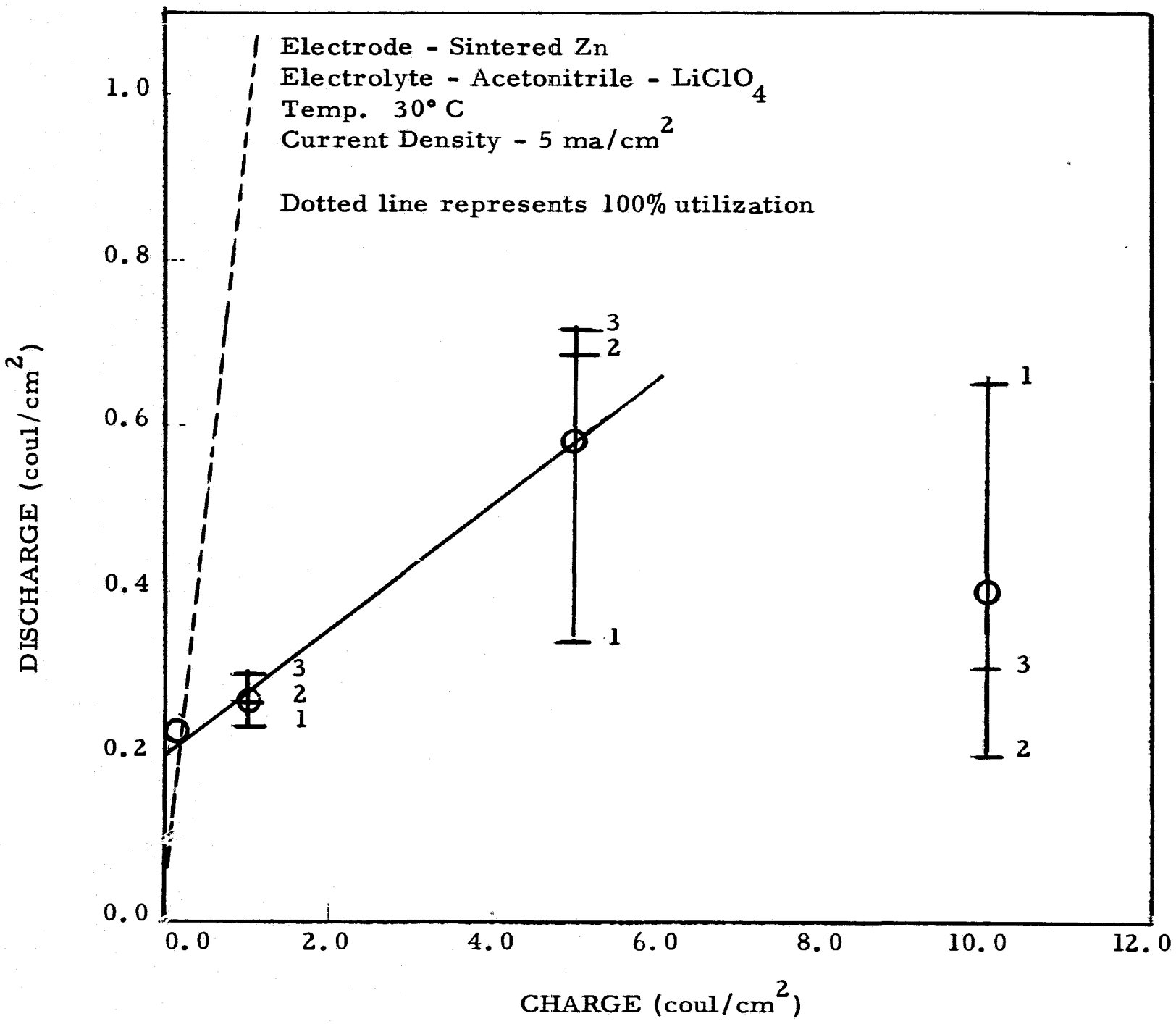


Figure 10. Coulombs delivered as a function of coulombs passed

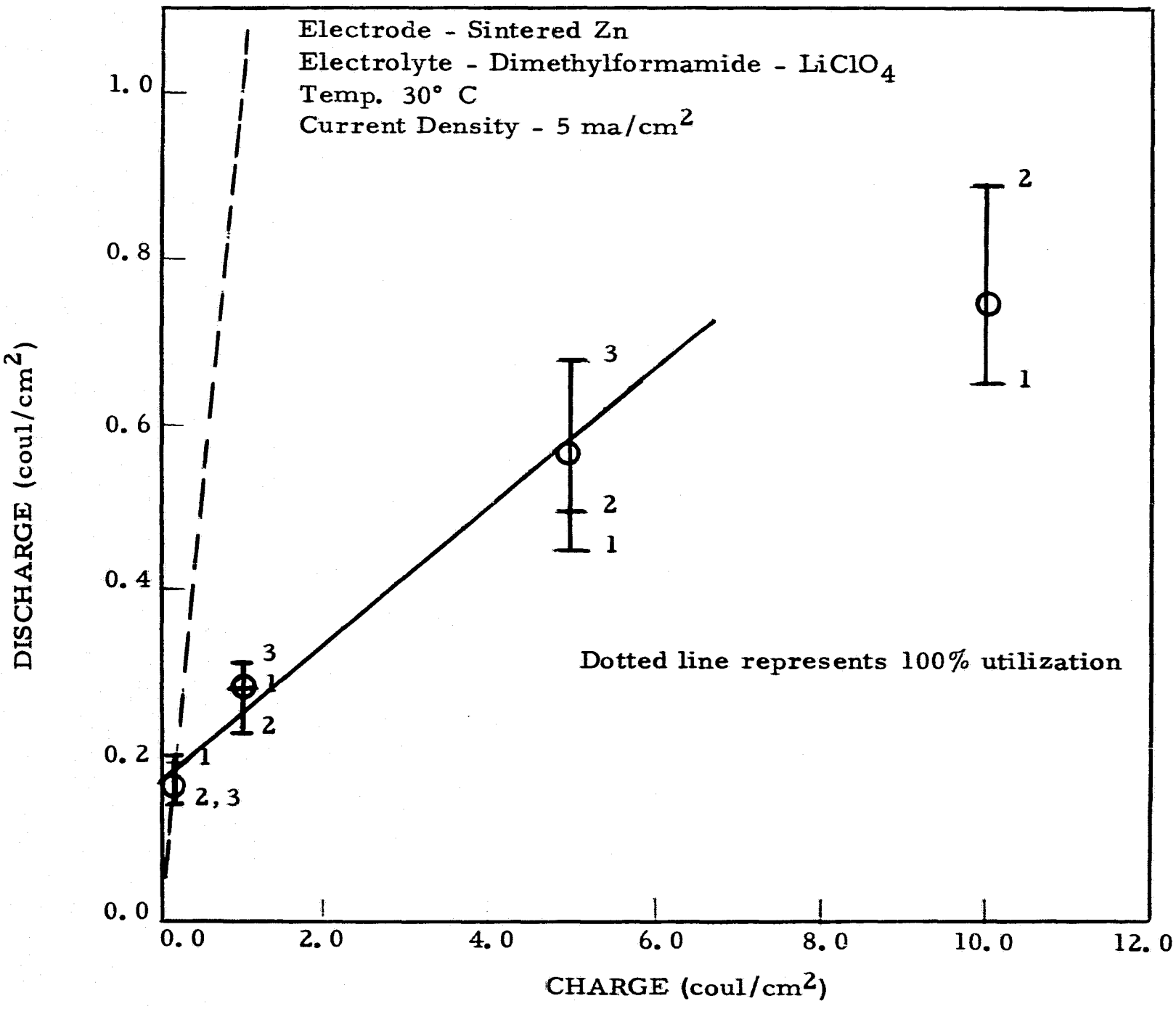


Figure 11. Coulombs delivered as a function of coulombs passed

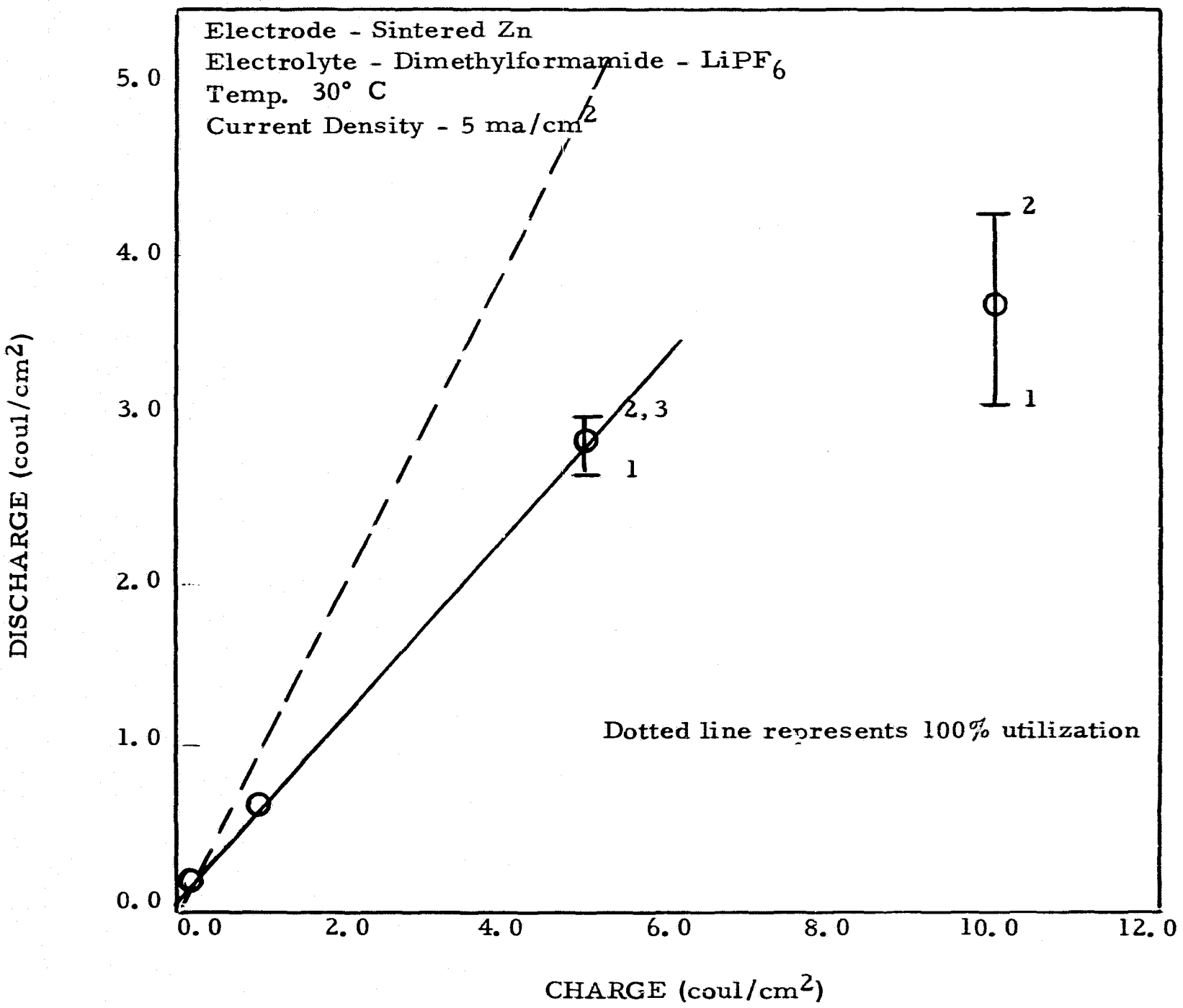


Figure 12. Coulombs delivered as a function of coulombs passed

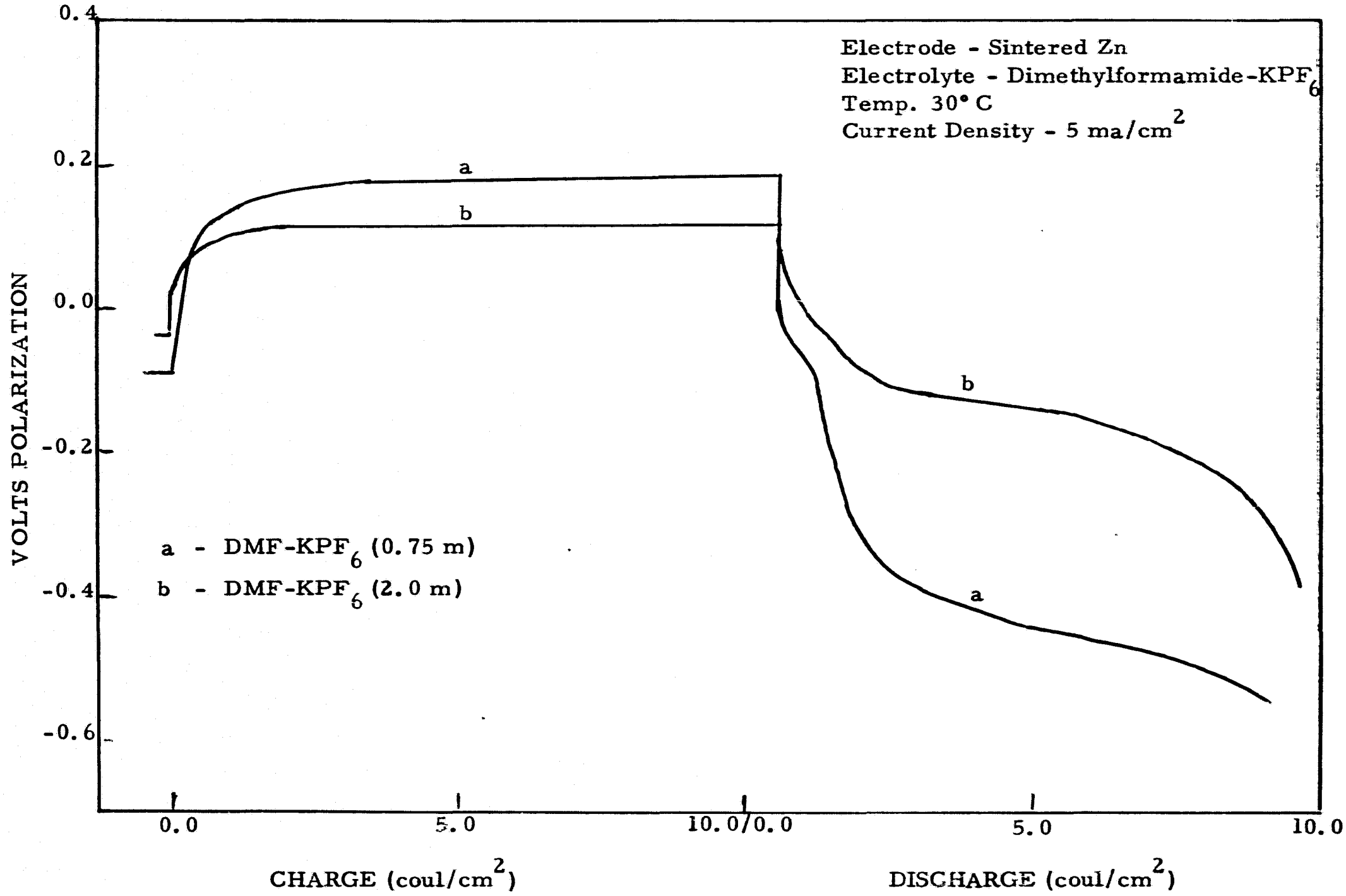


Figure 13. Charge and discharge curves for $Zn/DMF\text{-}KPF_6$

plots for these two systems as indicated in Figures 14 and 15. At the lower concentration (0.75 m) the utilization increases progressively with each cycle at the 5 coul/$cm^2$ charge input, having an average of 62% compared to 16% for the high concentration (2.0 m) where no significant cycling effect is noted. A cycling effect improves the utilization for the high concentration at the 10 coul/$cm^2$ charge input to an average of 42%. The utilization for the low concentration at 10 coul/$cm^2$ is 74%. A test at 5 coul/$cm^2$ on the high concentration system was made after the regular testing sequence had been followed and showed a utilization efficiency of 46%.

These data illustrate the significant effect of concentration, and of cycling, on utilization efficiency, and point out the importance of these factors in the optimum electroformation of high charge density positive plates. From this viewpoint the system is of interest.

## 13. Zinc Electrodes in Butyrolactone and Propylene carbonate-$KPF_6$

The systems Zn/Bl-$KPF_6$ and Zn/PC-$KPF_6$ behaved similarly. Both showed prolonged discharge at 1 ma/$cm^2$ (discharge capacity over 120% of the charge input) indicating reduction of dissolved material, and less than 15% utilization efficiency at 5 ma/$cm^2$ for charge inputs up to 5 coul/$cm^2$. The curves for this and lower charge inputs show relatively flat charging plateaus, followed by smaller polarized discharge (less than 1.0 coul/$cm^2$) with half-cell voltages dropping rapidly to greater than - 0.5 volts. The voltages separating the charge and discharge reaction are 0.2 and 6.0 volts for the Zn/BL-$KPF_6$ and Zn/PC-$KPF_6$ systems respectively. At the 10 coul/$cm^2$ charge input, a second apparently overlapping discharge becomes evident as seen in the discharge curves for the Zn/BL-$KPF_6$ system shown in Figure 16. The resulting enhancement in utilization efficiency at 10 coul/$cm^2$ charge can be seen in the charge-discharge plots for these two systems in Figures 17 and 18.

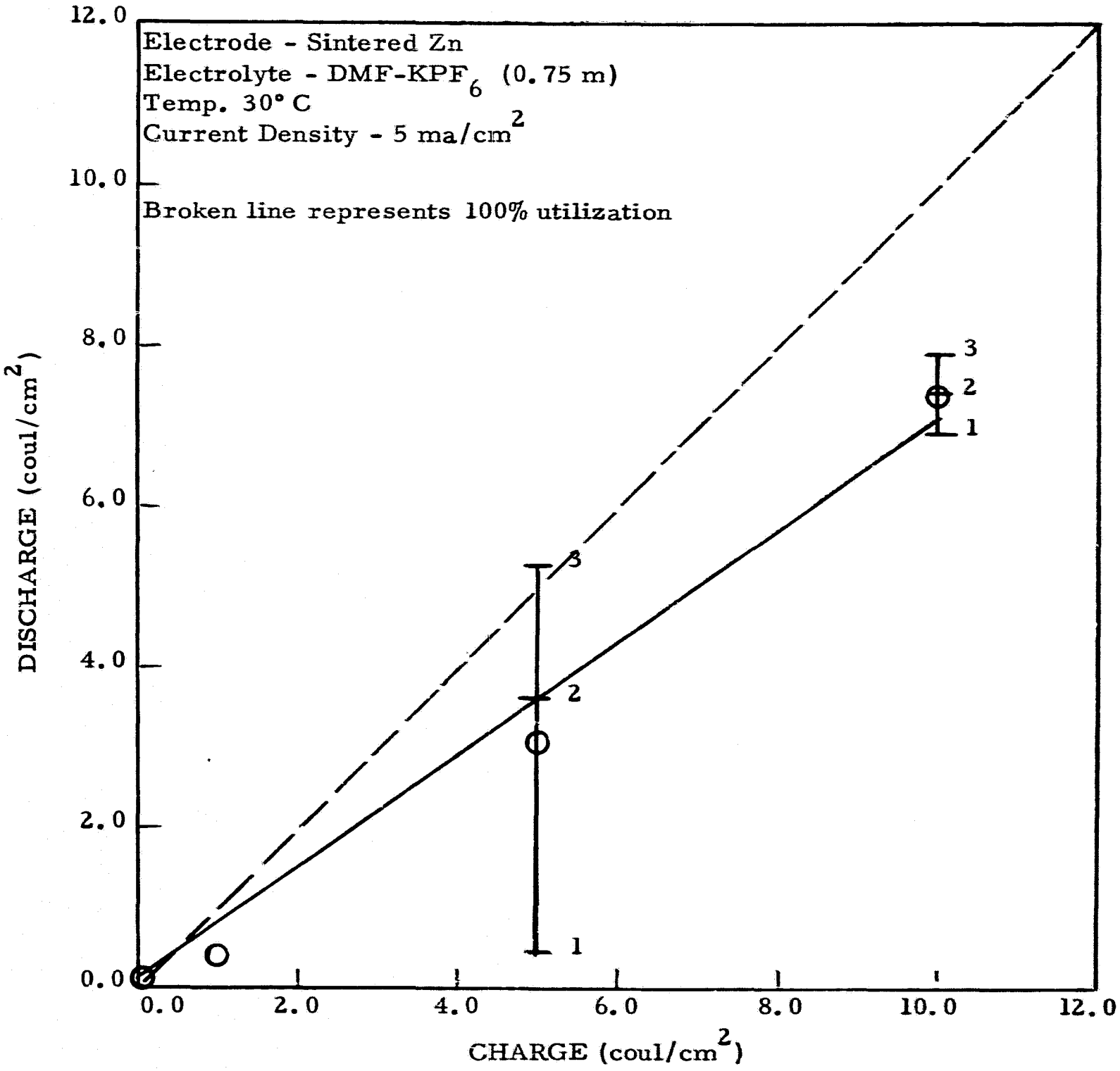


Figure 14. Coulombs delivered as a function of coulombs passed

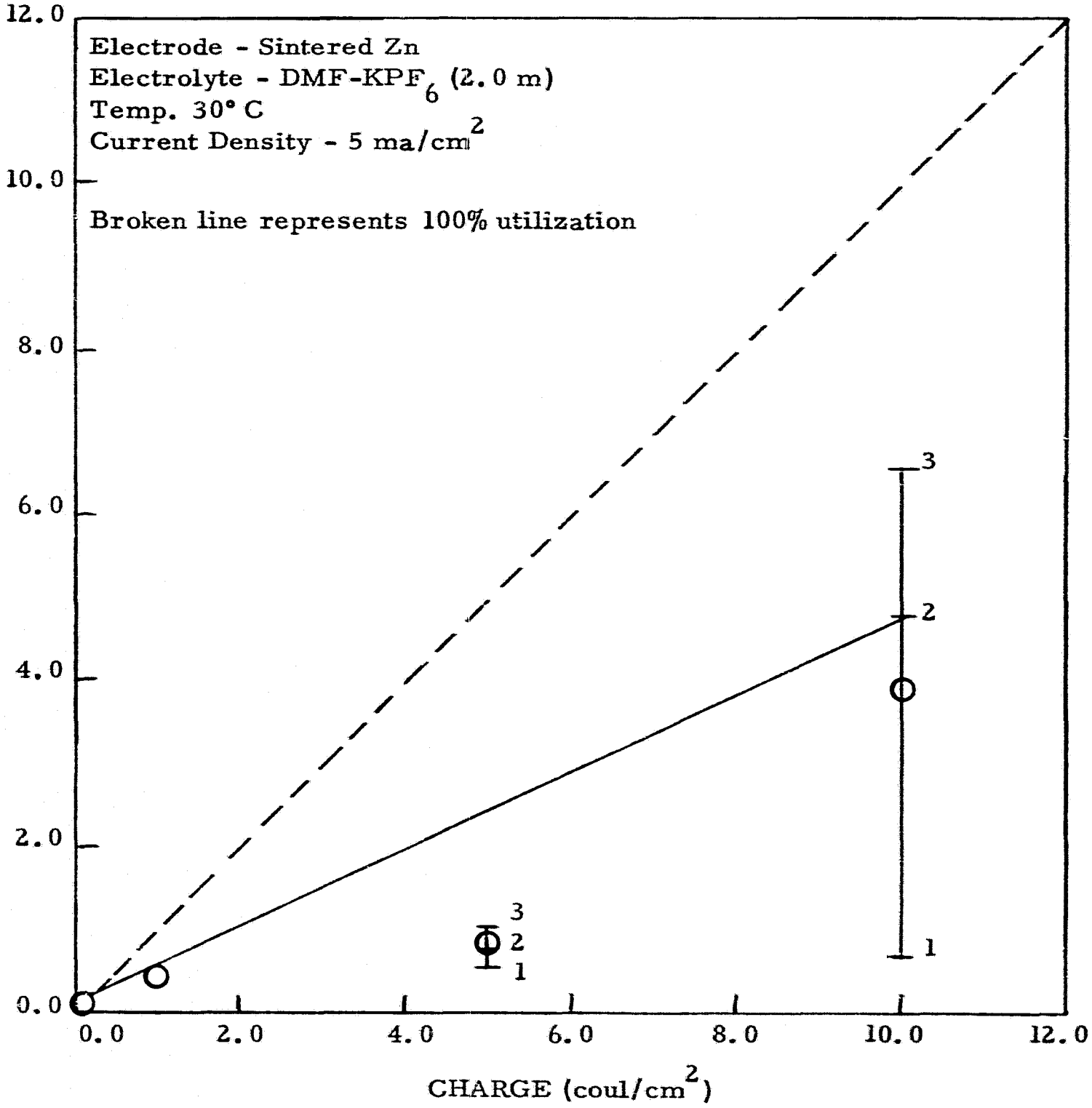


Figure 15. Coulombs delivered as a function of coulombs passed

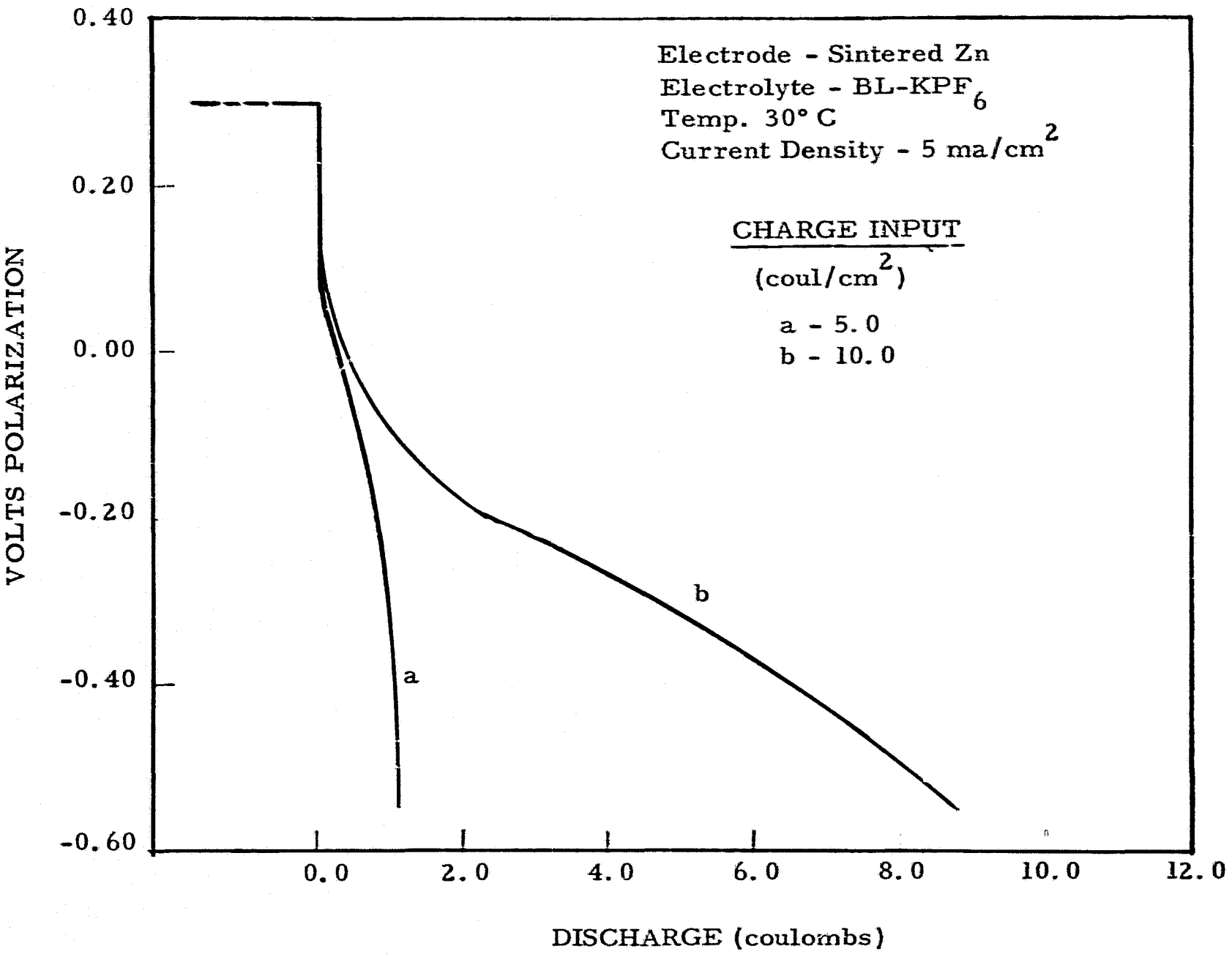


Figure 16. Discharge curve for $Zn/BL\text{-}KPF_6$

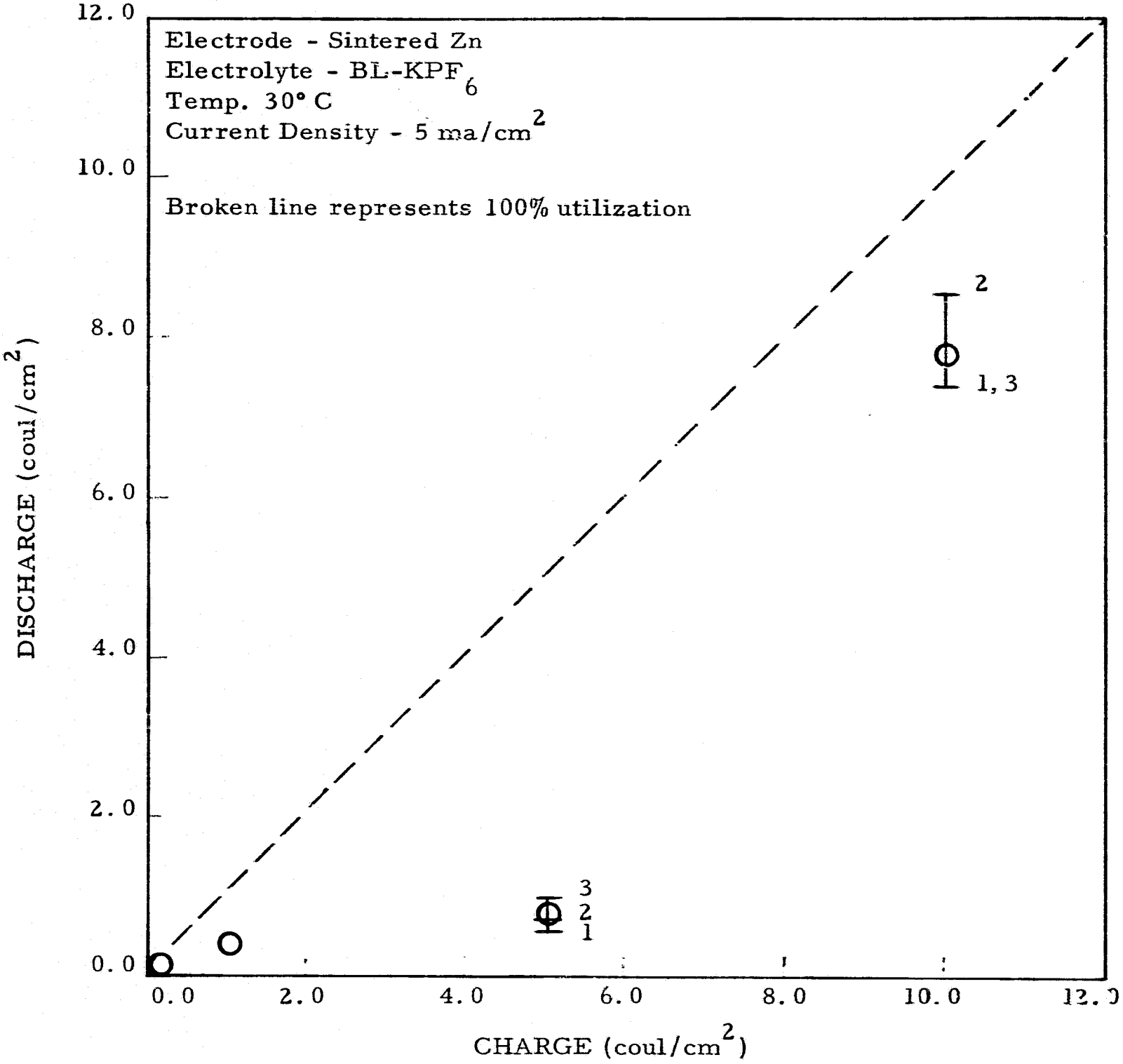


Figure 17. Coulombs delivered as a function of coulombs passed

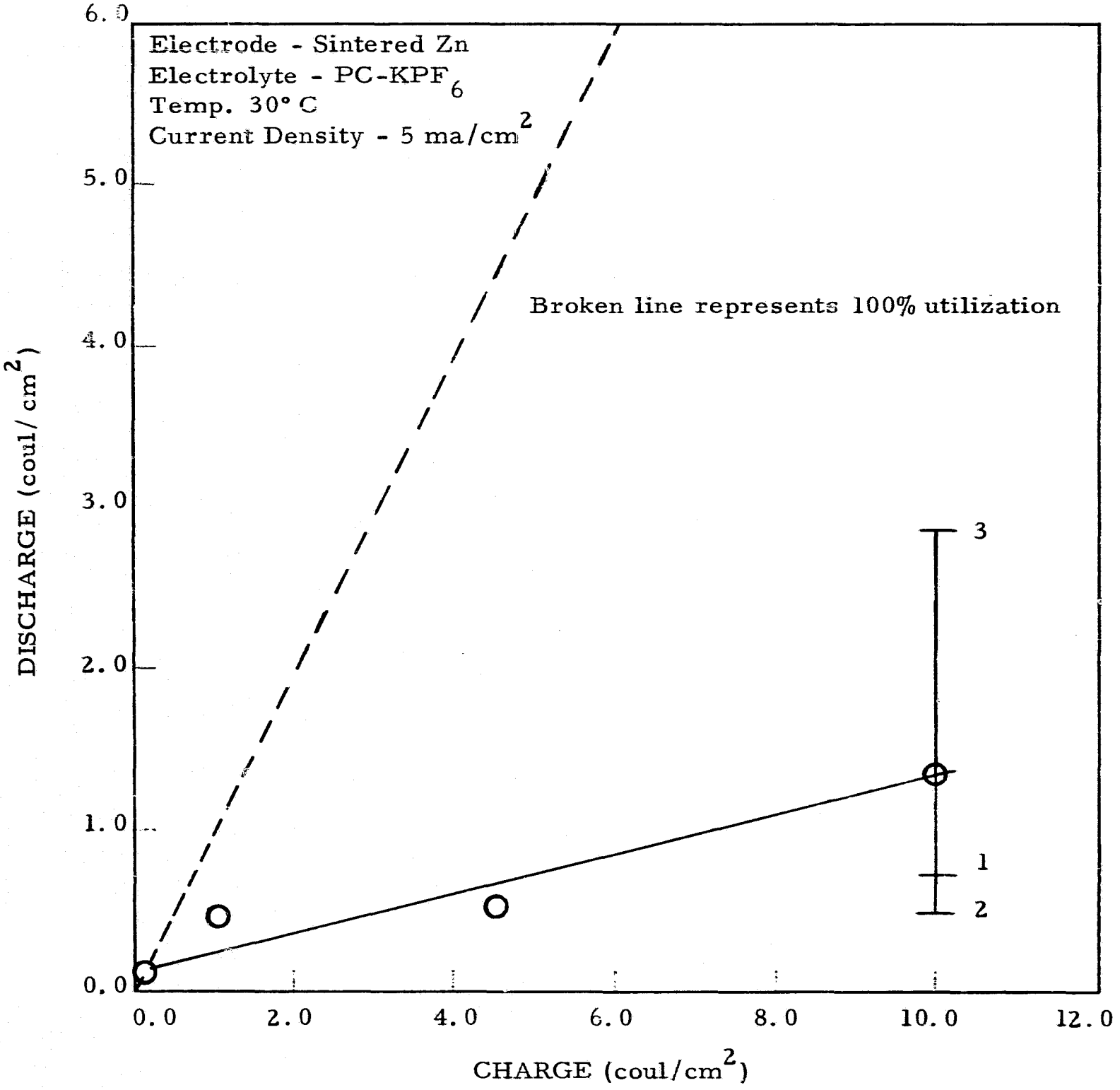


Figure 18. Coulombs delivered as a function of coulombs passed

The enhanced utilization at the 10 coul/cm$^2$ charge input may result from an increase in the effective porosity of the electrode, caused by the penetration of the charging reaction to deeper levels within the pores of the electrode, resulting in improved charge retention and utilization efficiency. Further tests are necessary at greater charge inputs to clarify these results.

## 14. Cadmium Electrode in Dimethylformamide-$KPF_6$

This system shows prolonged discharge for the 1 ma/cm$^2$ tests with low polarization between charge and discharge plateaus, indicating high electrochemical activity of dissolved material. The charge-discharge plot for this system at 5 ma/cm$^2$ is shown in Figure 19. Although the utilization efficiency is about 46%, taken up to 5 coul/cm$^2$, the discharge capacity at 10 coul/cm$^2$ of charge is greater than 100% indicative of discharge due to dissolved material. Examination of the working electrode revealed a build-up of a spongy grey material adhering to the electrode surface, which appears to represent a mixture of reduced metal and anodic product. It is likely that dissolution of this material near the electrode tends to raise the limiting current for reduction of dissolved active material.

Disposition of this system should be based on comparison with the other cadmium systems.

## 15. Cadmium Electrode in Dimethylformamide-$LiBF_4$

Sintered cadmium in DMF-$LiBF_4$ shows prolonged discharge at 1 ma/cm$^2$ with 0.03 v polarization between charge and discharge plateaus, indicating high electrochemical activity for dissolved material. The tests at 5 ma/cm$^2$ gave a small discharge plateau near 0.00 v which increased from 0.3 to 0.8 coul/cm$^2$ with cycling, followed by a second discharge plateau at - 0.07 v which did not drop off within 120% of the charge time. The charge-discharge

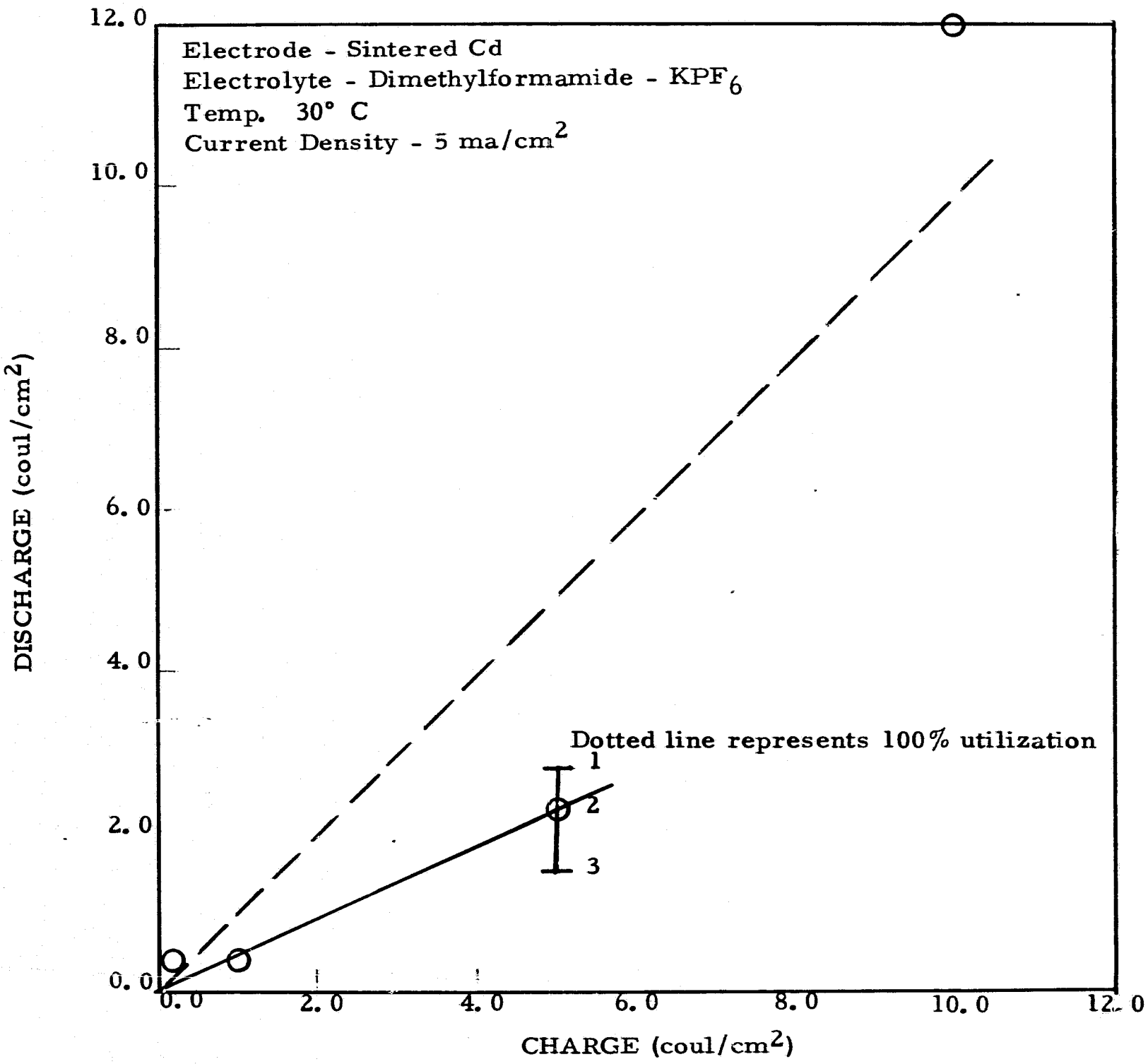


Figure 19. Coulombs delivered as a function of coulombs passed

plot for the first plateau is shown in Figure 20, representing a utilization efficiency of less than 15% for all charge inputs. The results indicate a low availability of solid material and a high availability of dissolved material at the electrode surface, which may result from a high dissolution rate of the electroformed product.

This system is not recommended for further testing.

## 16. Cadmium Electrode in Dimethylformamide-$LiClO_4$

The charge-discharge plot for this system is shown in Figure 21. A utilization efficiency of 53% is calculated from the best straight line through all points. The discharge at the lower charge inputs (0.10 and 1.0 coul/$cm^2$) is reproducible and falls within the circular points. At the higher charge inputs the spread of individual points among a given set is greater than 2 coul/$cm^2$. At 5 coul/$cm^2$, the lowest discharge is comparable to values obtained at the lower charge levels. The average utilization efficiency (calculated only for the largest charge input, 10.0 coul/$cm^2$) is 63%, a value greater than the average for all the tests. These effects may be explained as follows. The large spread at the higher charge level (10.0 coul/$cm^2$) can result from the expected formation of solid state material at deeper levels within the pores of the electrode where contact to the metal is favored, thus minimizing the relative significance of gross loss effects. It is expected on this basis, that this system and others with similar behavior, will show an improvement of the utilization efficiency at larger charge inputs (20-50 coul/$cm^2$).

This system is recommended for further consideration.

## 17. Cadmium Electrode in Butyrolactone-$KPF_6$

The discharge curve for the system Cd/BL-$KPF_6$ is shown in Figure 22.

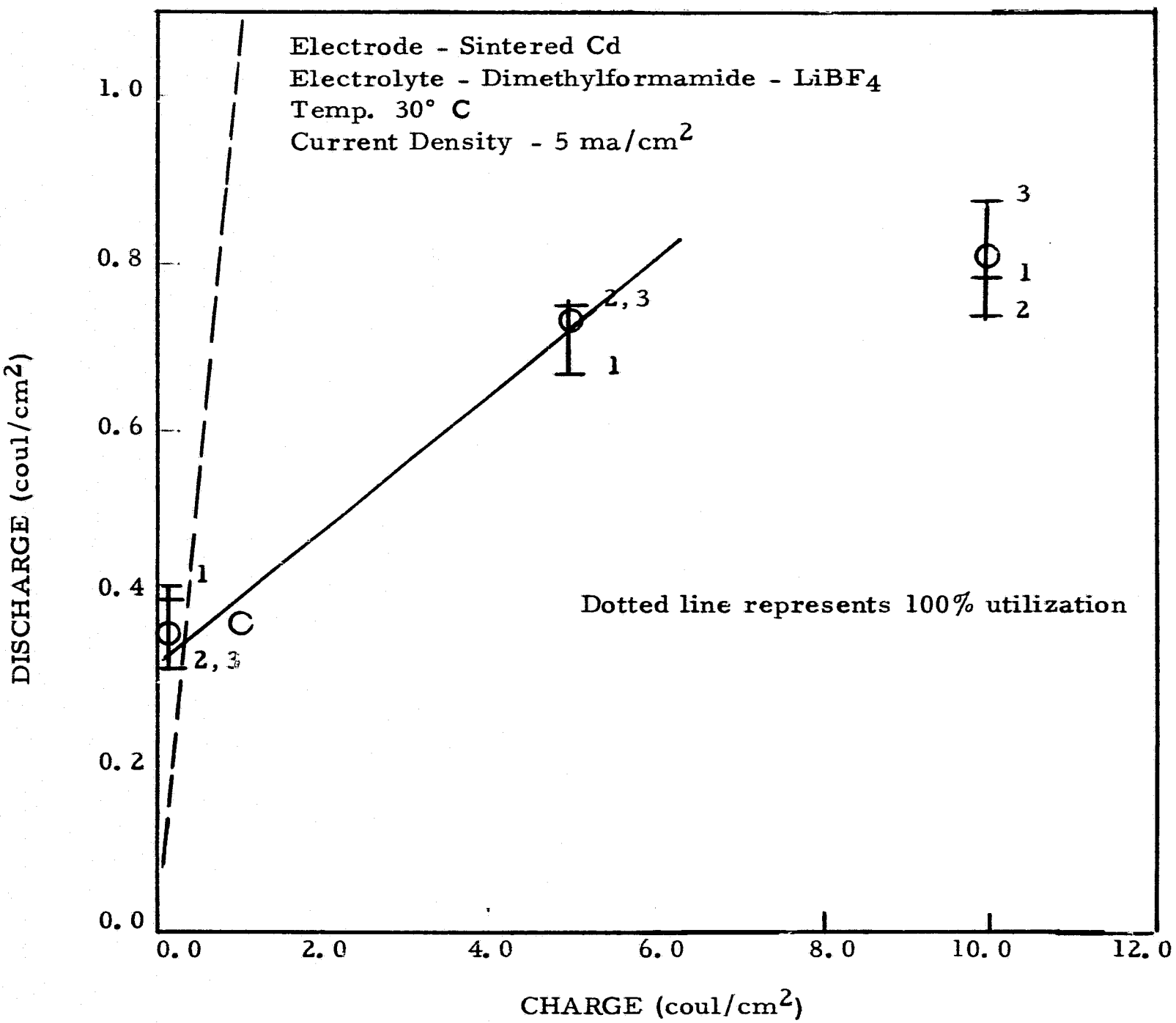


Figure 20. Coulombs delivered as a function of coulombs passed

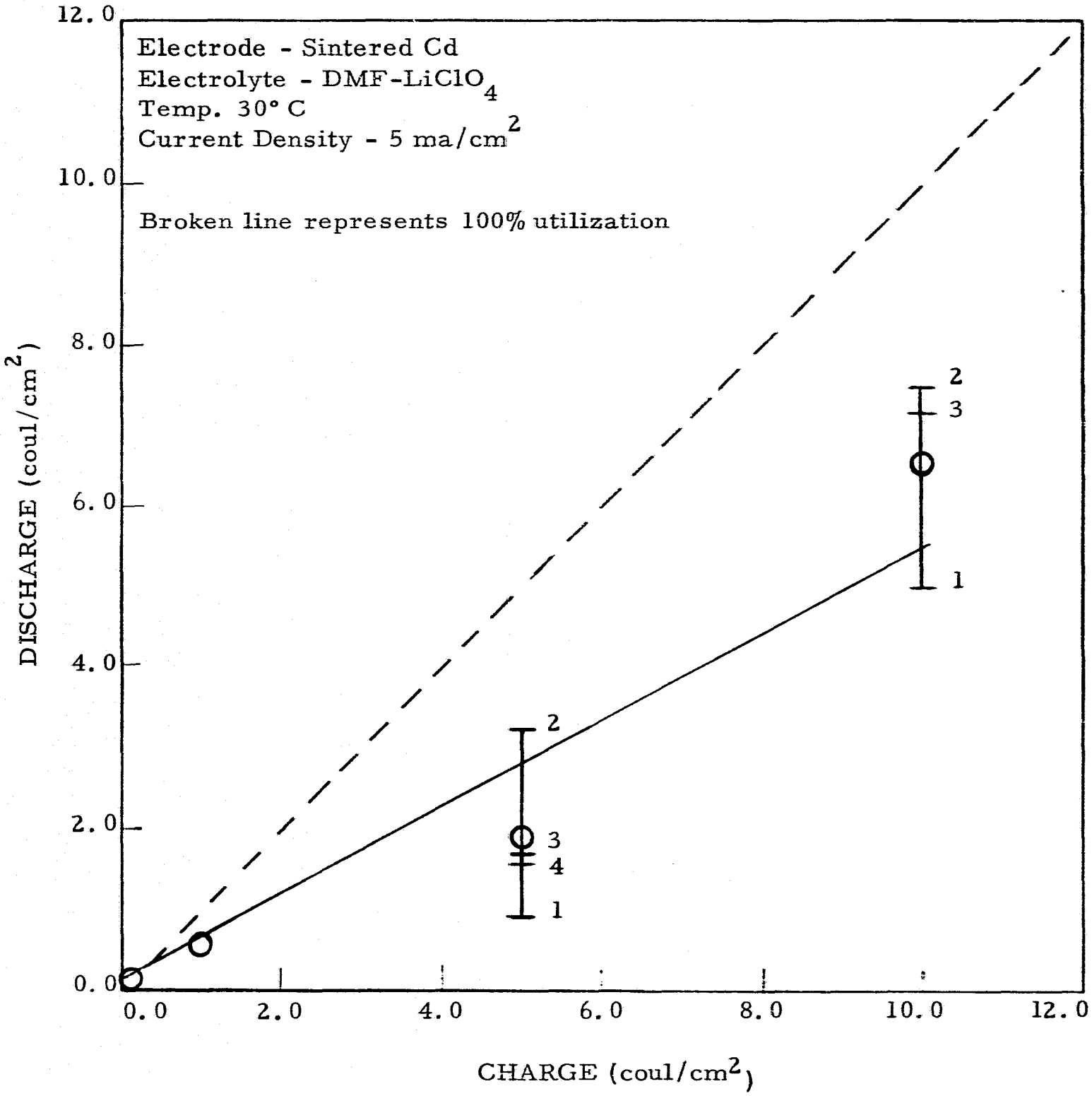


Figure 21. Coulombs delivered as a function of coulombs passed

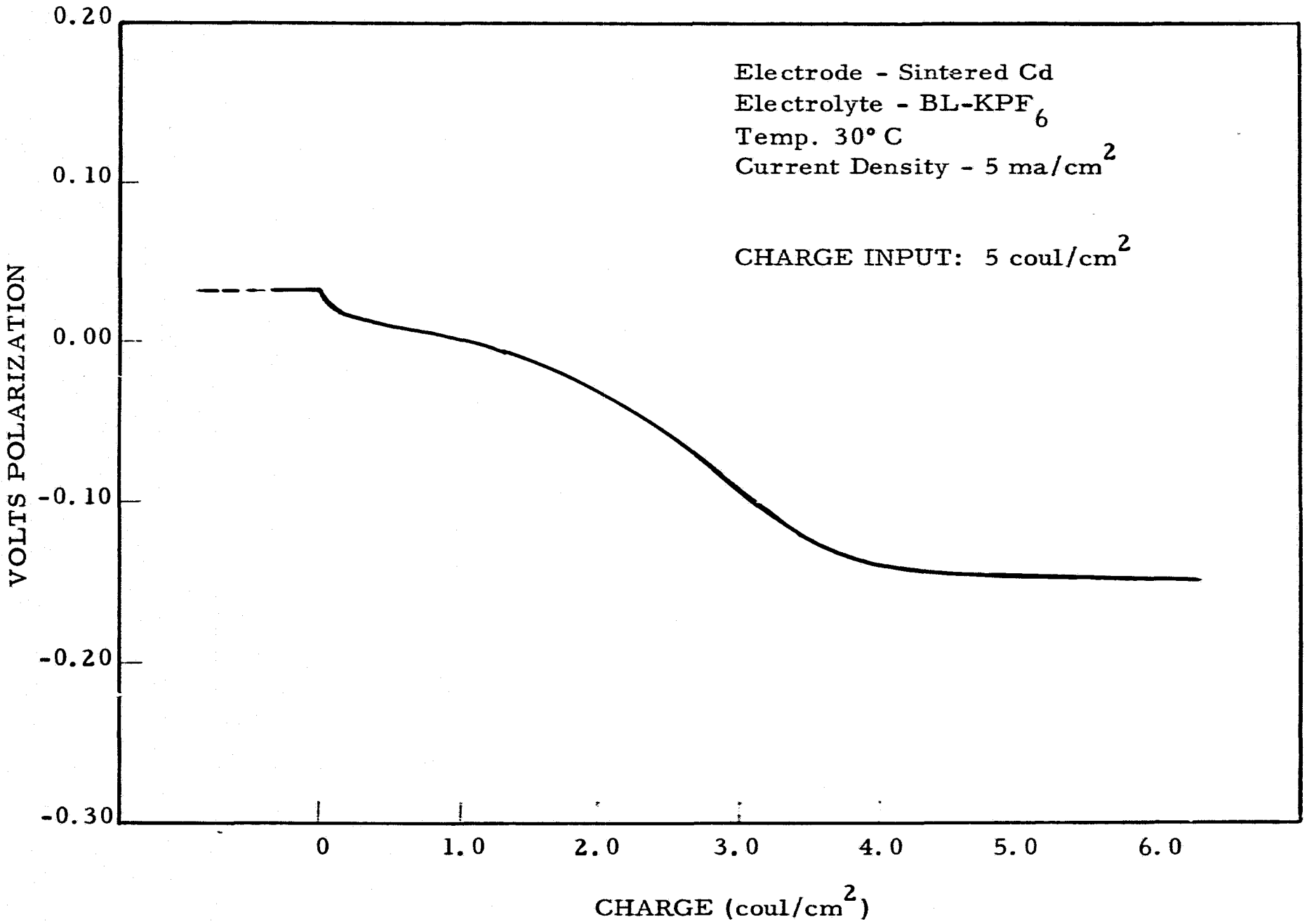


Figure 22. Discharge curve for Cd/BL-$KPF_6$

The curve shows very low initial polarization (50 mv) relative to the charge plateau, a portion of which is shown. The discharge plateau then drops gradually levelling off at - 120 mv, following which it continues until greater than the corresponding charge input. This effect is not evident in the discharge curves for the smaller charge inputs (0.10 and 1.0 coul/$cm^2$), where in fact a sharp break occurs with the discharge potential dropping rapidly to negative values greater than 0.5 volts vs the cadmium reference electrode. The charge-discharge plot for this system is shown in Figure 23, where the large spread for the discharge capacity at the 5 coul/$cm^2$ charge input, and the relative low utilization at 10.0 coul/$cm^2$ charge input, are evident.

It appears that in this system, loss of charged solid state material caused by gross effects, predominates during the charging process. The prolonged discharge at potentials slightly less than that for the solid state discharge is most likely caused by dissolved material. The appearance of the prolonged discharge for the larger charge inputs indicates an increase in the effective concentration of dissolved species possibly resulting from dissolution of solid material which builds up with cycling.

Consideration of further testing should be made relative to choice of the other cadmium systems.

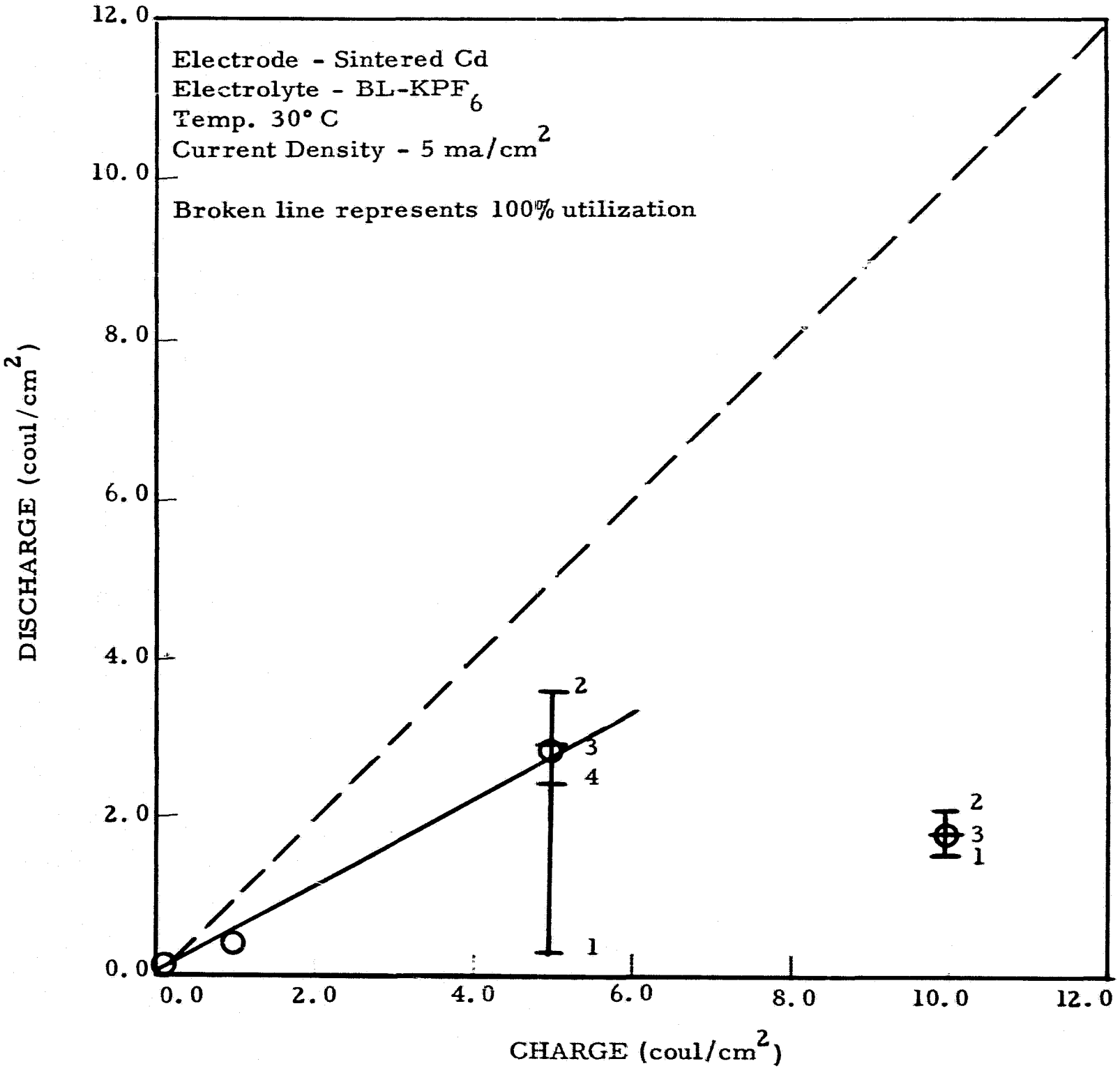


Figure 23. Coulombs delivered as a function of coulombs passed

# III. EXPERIMENTAL

## 1. Measuring Cell

Tests were conducted in a 3-compartment cell, with the working and reference electrodes positioned in the central compartment, and the counter-electrodes in the outer compartments. Cell dimensions were such as to provide at least a ten-fold excess of electrolyte to the working electrode at current densities well above those used in these tests. The cells were constructed from polypropylene sheets (3 x 2 1/2 x 1/8 inch) cut in appropriate shapes of sides and spacers, to form the compartments when assembled. The separate parts were fused together along the outer edges using a heat torch. The working electrode was positioned in the current path, provided for by 2.5 cm bore diameter holes in the spacers separating the working and counterelectrode compartments. Pyrex fritted, glass disks (Corning F) were affixed with a polypropylene melt onto the spacers to act as separators and retard diffusion of reaction by-products from the counterelectrode compartments.

## 2. Electrode Preparation

The working, counter, and reference electrodes consisted of the same metal for any given test. Porous, sintered, working electrodes were used. The zinc and cadmium electrodes were prepared by a chemosintering process, using - 100 mesh metal powder pressed onto nickel grids. Sintered copper felt electrodes were obtained from Huyck Metals Company. Standard silver plates from silver oxide - zinc batteries were provided by the Power Sources Division of Whittaker Corporation. These were charged to silver oxide in KOH at 2 ma/cm$^2$ to a specific capacity of 10 coul/cm$^2$ of electroactive material.

Silver fluoride, copper fluoride and copper chloride electrodes were

prepared by direct reaction of the metal with the active gas. The reaction was carried out in a closed system with pressure set at 30 psig (25° C), and with an argon-to-active gas ratio chosen so as to limit the extent of reaction to about 20 coul/cm$^2$, assuming complete reaction. Control electrodes, weighed before and after reaction, were used in all preparations to estimate the amount of reacted material per unit area on the electrode surfaces. In all cases the weight gain on the control electrodes corresponded to between 20 and 25 coul/cm$^2$. Counterelectrodes were made either from metal sheet or wire coils (total surface area = 100 cm). Reference electrodes consisted of the corresponding metal in wire form.

3. Electrolyte Saturation

All test solutions were saturated with respect to the corresponding electrode material. This was done in a two compartment H-cell by subjecting electrodes to a constant current of 10 ma/cm$^2$ for a minimum of three hours. This was more than sufficient to saturate the solutions, since the coulombs passed exceeded an equivalent value of 40 millimoles/liter, which is the cation concentration for the most soluble of the systems.

4. Electrode Preconditioning

Since it was not practical to sweep cycle the electrodes (due to electrode geometry and test cell setup), the electrodes were preconditioned by cycling the cell using a linearly varying current applied between the working and counterelectrodes. This current varied between 0 and ± 10 ma/cm$^2$ at a cycling frequency of 5 seconds per charge-discharge cycle. This frequency was chosen to maintain the polarization potential within ± 0.5 volts. Preconditioning was carried out for ten minutes prior to the charge-discharge tests. This was equivalent to 120 charge-discharge cycles.

## 5. Test Procedure

The charge-discharge tests consisted of galvanostatic charging at coulombic capacities of 0.1, 1.0, 5.0, and 10.0 coul/cm$^2$, and discharging to an appropriate cutoff voltage within 0.5 volts negative of the rest potential. Current densities of 1 and 5 ma/cm$^2$ were employed. Tests were started at the lowest coulombic input, then progressed to the larger charge capacity. A minimum of three tests were made for each charge capacity. Voltage-time curves were recorded during both the charge and discharge processes, measurements being made relative to a reference electrode. In cases of charged electrode systems, such as with the copper fluoride electrodes, a reduction current is applied to bring the electrode to an initial discharge state, then the regular procedure is followed.

# IV. REFERENCES

1. Whittaker Corporation, Narmco R and D Division, Eighth Quarterly Report, NASA Contract 38509, NASA CR-72419, May 1968.